Gene expression shifts in Emperor penguin adaptation to the extreme Antarctic environment

Josephine R. Paris* [1], Flávia A. Nitta Fernandes* [1,2], Federica Pirri [1,3], Samuele Greco [4], Marco Gerdol [4], Alberto Pallavicini [4], Marine Benoiste [2], Clément Cornec [2,5], Lorenzo Zane [3], Brian Haas [6], Céline Le Bohec [2,7,8], Emiliano Trucchi[$ 1]

* Joint First Co-Authors
$ Corresponding Author: Emiliano Trucchi (e.trucchi@univpm.it)

Affiliations

[1] Department of Life and Environmental Sciences, Marche Polytechnic University, Ancona, Italy
[2] Université de Strasbourg, CNRS, IPHC UMR 7178, Strasbourg, France
[3] Department of Biology, University of Padova, Padova, Italy
[4] Department of Life Sciences, University of Trieste, Trieste, Italy
[5] ENES Bioacoustics Research Laboratory, CRNL, CNRS, Inserm, University of Lyon, Saint-Etienne, France
[6] Broad Institute of MIT and Harvard, Cambridge, United States
[7] CEFE, Université de Montpellier, CNRS, EPHE, IRD, Montpellier, France
[8] Département de Biologie Polaire, Centre Scientifique de Monaco, Monaco, Principality of Monaco

Abstract

Gene expression can accelerate ecological divergence by rapidly tweaking the response of an organism to novel environments, with more divergent environments exerting stronger selection and, supposedly, requiring faster adaptive responses. Organisms adapted to extreme environments provide ideal systems to test this hypothesis, particularly when compared to related species with milder ecological niches. The Emperor penguin (*Aptenodytes forsteri*) is the only warm-blooded vertebrate breeding in the harsh Antarctic winter, in stark contrast with the less cold-adapted sister species, the King penguin (*A. patagonicus*). Assembling the first *de novo* transcriptomes and analysing multi-tissue (brain, kidney, liver, muscle, skin) RNAseq data from natural populations of both species, we quantified the shifts in tissue-enhanced genes, co-expression gene networks, and differentially expressed genes characterising Emperor penguin adaptation to extreme Antarctic ecology. Our analyses revealed the crucial role played by muscle and liver in temperature homeostasis, fasting and whole-body energy metabolism (glucose/insulin regulation, lipid metabolism, fatty acid beta-oxidation, and blood coagulation). Repatterning at the regulatory level appears as more important in the brain of the Emperor penguin, showing the lowest signature of differential gene expression but the largest co-expression gene network shift. Nevertheless, over-expressed genes related to mTOR signalling in the brain and the liver support their central role in cold and fasting responses. Besides contributing to understanding the genetics underlying complex traits, like body energy reservoir management, our results provide a first insight into the role of gene expression in adaptation to one of the most extreme environmental conditions endured by an endotherm.

Keywords: birds, cold adaptation, phenotypic plasticity, rapid adaptation, speciation, transcriptomics

Introduction

Organisms adapted to extreme environments provide ideal systems to study the evolutionary mechanisms that drive adaptation and speciation. Extreme environments are characterised by severe abiotic or biotic conditions that are challenging, or lethal, for most organisms to function in (Bell & Callaghan, 2012; Rothschild & Mancinelli, 2001). From an evolutionary perspective, the strong selective regimes imposed by such environments allow us to probe the fringe of biological resilience and evolutionary innovation, and, more generally, the causes and consequences of adaptive evolution (Grant et al., 2017; Hoffmann & Hercus, 2000; Hoffmann & Parsons, 1997). Comparison of these highly specialised organisms to ancestral lineages, or sister species, occupying milder environments, provides a powerful framework to understand the evolutionary processes that mediate organismal function under adverse environmental conditions (Tobler et al., 2018).

A predictably extreme environment (*sensu* Wingfield et al., 2011), such as a desert, a polar or an alpine region, is one outside an ancestral species' centre of distribution or environmental envelope (Bell & Callaghan, 2012), which represents a vacant niche that the ancestral species must colonise (Chapin et al., 1993; Chesson & Huntly, 1997; Jackson et al., 2009; Lekevičius, 2009). In such a scenario, we can predict strong selection and rapid adaptation (Chevin & Hoffmann, 2017; Grant et al., 2017). Compelling examples include rapid adaptation to temperature extremes in *Drosophila* (Hoffmann et al., 2003), and microbial adaptation to UV irradiation, extreme pH, and salinity (Wani et al., 2022). Amongst vertebrates, support for rapid adaptation to extreme environments has been evidenced in sheep following domestication to plateaus and deserts (8-9 kya; Yang et al., 2016), and polar bears to the extreme cold of the Arctic (400 kya; Liu et al., 2014). Characterising the evolutionary processes contributing to the physiological, metabolic, morphological and life cycle adaptations to extreme environments could therefore also enhance our predictions for describing the capacity of organisms to respond to the rapidly changing conditions of the Anthropocene (Botero et al., 2015; Chevin et al., 2010).

Rapid adaptive responses to extreme environments can be achieved through plastic or genetic evolutionary changes (or a combination of the two). For the latter, rapid adaptation most frequently occurs via polygenic standing genetic variation (Pfenninger et al., 2023; Yeaman, 2015). But how much does plasticity favour rapid adaptation to an extreme environment? Phenotypic plasticity is heritable (Scheiner & Lyman, 1989) and can increase the likelihood of survival under extreme conditions by accelerating the pace of evolution by fine-tuning an organisms' genetic repertoire (Levis & Pfennig, 2016; Scheiner, 1993; Via & Lande, 1985). In particular, gene expression links the genotype and phenotype and is shaped by both environmental and genetic factors (Pavey et al., 2010). Expression patterns can evolve in response to differential selection between environments (Fay & Wittkopp, 2008; Whitehead & Crawford, 2006), where the diversity of cellular functions is achieved through the expression of individual genes orchestrated by large, layered regulatory networks (Davidson & Erwin,

2006; Wittkopp, 2007). Therefore, if gene regulation is indeed important in shaping adaptation to extreme environments (see Hoffmann & Parsons, 1997), we expect the signal of gene expression divergence to be more related to the specific phenotypes of the focal species, than to broader biological processes governing the biology of both species.

A model that can be used to test these expectations is the case of the Antarctic Emperor penguin (*Aptenodytes forsteri*) and the sub-Antarctic King penguin (*Aptenodytes patagonicus*). Despite having diverged ca. 100,000 generations ago (Bird et al., 2020; Gavryushkina et al., 2017), the two species show clear morphological and behavioural differentiation as a consequence of ecological adaptation to totally divergent temperature regimes. The Emperor penguin completes its breeding cycle at temperatures below -45°C with winds of up to 50 metres a second, whilst the King penguin breeds in the ice-free and more temperate climates of the sub-Antarctic islands, where temperatures rarely fall below -5°C (Kooyman, 1993; Le Maho, 1977a; Prévost, 1961). Fossil evidence, paleoclimatic reconstructions, and ancestral niche construction suggest that whilst all penguins are birds of cold temperate to subtropical environments, the Emperor penguin represents the furthest evolutionary state of cold adaptation (Pirri et al., 2022; Simpson, 1946, 1976; Stonehouse, 1969; Vianna et al., 2020). Consequently, as the sister species, the King penguin more closely resembles the ancestral state of *Aptenodytes* penguins (Pirri et al., 2022).

To withstand the harsh environmental conditions of Antarctica, the Emperor penguin hosts a suite of remarkable physiological and behavioural adaptations. Being the largest extant penguin species, with a body mass ranging from 20-40 kg (the King penguin weighs approximately half this: 10-20 kg), its extensive subdermal body fat provides both insulation and energy reserves (Groscolas & Robin, 2001; Le Maho et al., 1976). Heat conservation is also highly optimised via advanced feather and plumule structure and distribution (Williams et al., 2015), and counter current arterio-venous heat exchangers (Thomas et al., 2011). Behavioural adaptations, such as huddling (Ancel et al., 1997; Gilbert et al., 2006), are also crucial for emperor penguins to protect themselves against the extreme cold and to lower energy expenditure. Moreover, emperor penguin reproduction is associated with a period of prolonged fasting: up to 45 days for adult females and four months for adult males (Ancel et al., 1992). These fasting periods are associated with metabolic adaptations to provide an optimal management of energy resources, including the maintenance of stable plasma glucose concentrations, moderate plasma-free fatty acids, and modest ketosis (Groscolas & Leloup, 1986; Groscolas & Robin, 2001). In addition, the reproductive, moulting, and fasting cycles of the Emperor penguin have to be completed during the dramatic photoperiodic cycles of Antarctica (Miché et al., 1991).

Here, we investigate the role of gene expression in adaptation to the extreme Antarctic environment in the Emperor penguin, by evaluating gene expression patterns across five tissues: brain, kidney, liver, muscle, and skin, collected from 10 wild chicks of both the Emperor penguin and the King penguin. Our sampling concerned tissues that we

hypothesised would exhibit the major gene expression differences for cold adaptation: brain (cold tolerance, circadian rhythm, huddling behaviour), kidney (osmoregulation, excretion of metabolic waste products), liver (lipid and fatty-acid metabolism), muscle (thermogenesis), and skin (feather development and thermal insulation). After generating the first transcriptomes of both species, we asked: 1) What is the role of species-specific tissue-enhanced transcripts in adaptation?; 2) What is the biological function of Emperor penguin-specific networks of genes?; 3) What are the biological functions of tissue-specific differentially expressed genes in the Emperor penguin?

2. Materials & Methods

2.1 Sample collection

Emperor and King penguin individuals were sampled from natural populations between June and September 2016. Emperor penguins were sampled from a colony of *Pointe Géologie* close to the Dumont d'Urville Station in Adélie Land, Antarctica. King penguins were sampled from the colony *La Baie Du Marin*, close to the Alfred Faure Station in Possession Island, Crozet Archipelago (Figure S1). All procedures employed during field work were approved by the French Ethical Committee and the French Polar Environmental Committee, and authorisations to enter the breeding site and to collect samples from dead birds were delivered by the “Terres Australes et Antarctiques Françaises” (permit nos 2015-52 and 2015-105). Ten chicks (aged between 3-7 months) were sampled for each species. For each individual, five tissues (brain, kidney, liver, skin, and muscle) were sampled for a total of 100 samples (50 samples per species). All tissue samples were collected from freshly predated chick corpses (Table S1). Although predation stress and the exact time from death may have affected gene expression, major expression profiles should have been preserved by the timely collection of tissues. Tissues were dissected and chopped into pieces ~4 mm, which were directly fixed in RNAlater (Applied Biosystems, UK) and stored at −80°C.

2.2 RNA extraction, library construction, and sequencing

For brain, kidney and liver tissues, total RNA was isolated using a standard TRIzol-chloroform protocol. RNA extraction from skin and muscle tissue using this method resulted in poor RNA yields. Total RNA for these tissues was therefore extracted using the RNeasy Fibrous Tissue Mini Kit (Qiagen, Germany) according to the manufacturer’s instructions. RNA purity and concentration was assessed using a Nanodrop 2000 (Thermo Fisher Scientific, CA) and a Qubit 4.0 fluorometer (ThermoFisher Scientific, CA), respectively. RNA integrity (RIN) was evaluated by UV transilluminator and Agilent 2100 Bioanalyzer (Agilent technologies, CA), accepting a RIN score >6 for library preparation.

For the construction of sequencing libraries aimed at *de novo* transcriptome assembly, the total RNA samples extracted from five tissues (brain, kidney, liver, muscle, skin) in three individuals of each species, were pooled in equimolar concentrations. This resulted in a total

of three RNA pools for each species. Library preparation and sequencing was carried out by BMR Genomics Service (Padova, Italy). Libraries were synthesised using the Illumina TruSeq Stranded mRNA Sample Prep kit. Poly-A mRNA was fragmented for 3 minutes at 94°C, and each purification step was carried out with 1 × Agencourt AMPure XP beads. Paired-end sequencing (100bp x2) was performed on an Illumina NovaSeq 6000 at a targeted sequencing depth of 20 million reads per library.

For the analysis of gene expression, library preparation was performed using the QuantSeq 3'mRNA-Seq Library Prep Kit FWD V1 (Lexogen, Vienna, Austria), using the total RNA extracted from the five aforementioned tissues in individual penguins. QuantSeq provides an accurate method for gene expression (even at low read depths) by generating only one fragment per transcript, making the number of reads mapping to a gene proportional to its expression (Corley et al., 2019; Moll et al., 2014). Individual libraries were barcoded and pooled for sequencing on an Illumina NextSeq500 (single-end, 75bp) at a target sequencing depth of 5 million reads per library.

2.3 *De novo* transcriptome assembly and annotation

Read quality was examined using FastQC v0.11.9 (Andrews, 2010). Trimming was performed using fastp v0.20.1 (Chen et al., 2018), enabling the elimination of homopolymer tails. Sequences < 71bp were discarded. Transcriptome assembly for each species was performed using the Oyster River Protocol (ORP) v2.2.5 (MacManes, 2018). By taking advantage of the strengths of different assembly tools, the ORP method recovers transcripts that may be missed by individual assemblers and minimises redundancy, improving overall assembly quality. Within ORP, trimmed reads were error corrected using Rcorrector v1.0.4 (Song & Florea, 2015). Reads were then assembled using three different *de novo* assemblers and different *k*-mer sizes: Trinity v2.11.0 with 25-mers (Grabherr et al., 2011; Haas et al., 2013), rnaSPAdes v3.14.1 with both 55-mers and 75-mers (Bushmanova et al., 2019), and Shannon v0.0.2 with 75-mers (Kannan et al., 2016). Contigs that were expressed at less than 1 transcript per million (TPM) reads were removed. This resulted in four distinct assemblies that were merged and clustered into isoform groups using OrthoFuse within ORP. The resulting assembly was used as input to TransRate v1.0.3 (Smith-Unna et al., 2016), and the best transcript (in regard to highest contig score) from each group was placed in a new assembly file to represent the entire group. Only transcripts >250bp were retained. We removed contigs derived from ribosomal and mtDNA from the assembly (Text S1).

The overall quality of the assemblies was evaluated with BUSCO v5.2.2 (Simão et al., 2015), using the Aves (n=8782) OrthoDB v10 database (Kriventseva et al., 2019). We also used TransRate v1.0.3 (Smith-Unna et al., 2016) to further assess completeness. The Ex90N50 statistic was quantified as a measure of contiguity, where the N50 value is computed based on the top 90% of transcripts based on expression levels (Haas et al., 2013). Expression levels were estimated by mapping the trimmed reads used for the assembly back to the assembled

transcripts using Salmon v1.10.2 (Patro et al., 2017) and statistics were calculated using the TrinityStats.pl script (Haas et al., 2013).

The Trinotate software (github.com/Trinotate/Trinotate/wiki, v4.0.1) was used to annotate the transcriptomes and predict coding regions. First, coding regions were predicted within using TransDecoder (github.com/TransDecoder/TransDecoder/wiki, v5.7.1). The transcript sequences and predicted peptides were used as input to Trinotate for automated functional annotation including identification or protein domains (HMMER v3.1; Finn et al., 2011) search of Pfam v35 (Finn et al., 2014), top BLASTP and BLASTX match to SwissProt (Release 2023_03 searched using DIAMOND; Buchfink et al., 2021), signal peptides via SignalP v6.0 (Teufel et al., 2022), transmembrane domains via TMHMM v2.0c (Krogh et al., 2001), noncoding RNA genes using Infernal v1.1.4 (Nawrocki & Eddy, 2013), and additional functional annotations captured from eggNOG-mapper v2.1.9 (Cantalapiedra et al., 2021). Long non-coding RNAs (lncRNAs) are unlikely to produce proteins but they may still play a key role in eukaryotic gene regulation (Mattick et al., 2023). We therefore also generated catalogues of lncRNAs for both species (see details in Text S2; available on GitHub: Paris et al., 2023).

2.4.1 Transcript mapping to *de novo* transcriptomes

Raw QuantSeq reads were cleaned using bbduk in BBmap v39.01 (Bushnell, 2014) with parameters specific to 3' QuantSeq data (Text S3). Quality was assessed using FastQC (Andrews, 2010). Trimmed reads from each species were mapped to the respective transcriptome using Salmon v1.10.2 (Patro et al., 2017), to perform transcript-level abundance estimation, setting the mapping parameters for 3' QuantSeq data (Text S3). Raw counts were filtered to remove transcripts with low counts (<10 reads in at least 9 or 10 samples in the Emperor penguin and King penguin groups, respectively - one Emperor penguin sample was removed; see Results). This filter reduced our raw table of transcript counts to 21,977 in the Emperor penguin and to 22,793 in the King penguin.

2.4.2 Analysis of tissue-enhanced transcripts (TEGs)

Analysis of tissue-enhanced transcripts was performed using DESeq2 in R (Love et al., 2014), specifying '~ Tissue' as the negative binomial GLM formula. To quantify tissue-enhancement, contrasts were performed on the counts of each target tissue versus the mean counts of all other tissues. An FDR threshold < 0.01 and a log2foldchange ≥ 5 used to determine significant tissue-enhanced transcripts (*sensu* Sjöstedt et al., 2020; proteinatlas.org/humanproteome/tissue/tissue+specific) and ≤ -5 as tissue-inhibited transcripts (significantly lower in a particular tissue compared to the average level in all other tissues). To explore the patterns of tissue-enhanced and -inhibited transcripts in each species, we visualised patterns of enhancement or inhibition using the Variance Stabilising Transformation (VST) normalised counts. To identify species-specific tissue-enhanced genes (TEGs), tissue-enhanced transcripts were intersected with the transcriptome annotation to identify putative transcript function (therefore referred to as genes). To explore the biological processes of the

species-specific genes, we performed Gene Ontology (GO) enrichment analysis on the Biological Process (BP) categories using the *enricher* function in clusterProfiler v4.8.2 (Yu et al., 2012), using a minimum gene size of 10 and a maximum gene size of 500 and an FDR ≤ 0.05 to test for significance. For both species, genes annotated with Trinotate with associated GO IDs (17,874 in the Emperor penguin and 17,098 in the King penguin) were used as a background.

2.5.1 Transcript mapping to the Emperor penguin genome

For analysis of regulatory networks and differential gene expression, we aligned the Quantseq data of both species to the Emperor penguin genome (GCF_000699145.1; Li et al., 2014). Note that attempts at reciprocal transcript mapping between the Emperor and King penguin transcriptomes suffered from incomplete isoform resolution. The Emperor penguin genome was chosen because it displayed improved assembly statistics and a higher number of annotated protein-coding genes in comparison to the King penguin genome (Table S2). Trimmed sequencing reads were aligned using STAR v2.7.9a and counted with htseq-count v0.11.3 with parameters specific to QuantSeq data (Text S3). The raw table of gene counts including samples from both species was filtered to remove genes with <10 reads in at least 9 samples of each tissue (reducing the table of gene counts from 15,333 to 10,797 for the King penguin and Emperor penguin, respectively). Clustering of the biological replicates of each of the five tissues was assessed using the VST-normalised count data via Principal Component Analysis (PCA).

2.5.2 Analysis of co-expression modules

Construction of co-expression modules was performed using weighted gene co-expression network analysis (WGCNA; Langfelder & Horvath, 2008). We kept the upper 75th quantile of the normalised count data from the alignment to the Emperor penguin genome, resulting in a dataset of 2699 genes. All samples and genes passed the missing data filter implemented using the default parameters in the *goodSamplesGenesMS* function.

Gene co-expression networks were constructed for both species using the *blockwiseModules* function. In weighted co-expression networks, genes (network nodes) are connected by the pairwise correlation of their expression (network edges) in an adjacency matrix. In WGCNA, the adjacency (correlation) matrix is raised to a power $\beta \geq 1$ (soft thresholding), so that high correlations are accentuated over low correlations (Zhang & Horvath, 2005). We designated a soft threshold value β of 12 for both the Emperor penguin and King penguin adjacency matrices, corresponding to the value for which the scale-free topology model fit (R^2) stabilised with increasing power (Figure S2). Co-expression modules for each species were defined through the Topological Overlap Measure (TOM) of their respective adjacency matrices, with dissimilarity based on hierarchical clustering. The resulting gene dendrogram was trimmed using the dynamic tree-cutting method (Langfelder & Horvath, 2008), generating modules with at least 30 genes. Modules with correlations higher than 0.25 were merged.

To associate co-expression modules to the five different tissues, we defined the first principal component (PC1) of each module's gene expression profile, also known as the module eigengene (ME) (Langfelder & Horvath, 2008). The correlation between the MEs and the tissue samples was tested using a Pearson correlation (*cor* function), with p-values determined using a Student's asymptotic test (*corPvalueStudent* function).

Co-expression modules from a reference species that are not preserved in a test species can be indicative of regulatory novelties in the reference group (Oldham et al., 2006). We therefore tested if co-expression modules defined in the network of the Emperor penguin (reference network) were also preserved in the King penguin (test network). Gene density and connectivity statistics were calculated using the *modulePreservation* function, outputting a series of preservation statistics (see Langfelder et al., 2011 for detailed information). The significance of each preservation statistic was validated through random permutation tests (Langfelder et al., 2011).

To interpret the potential biological function of the genes within our chosen modules (*i.e.*, the Emperor penguin specific modules, *a.k.a.* the least preserved modules in the King penguin network), we performed a GO enrichment analysis. We used the chicken (*Gallus gallus*) gene sets and related GO terms as a starting point, which were downloaded from Ensembl using biomart v2.56 in R. Intersecting this database with the Emperor penguin genome annotation (14,572 protein-coding genes), we harnessed 66,367 Biological Process (BP) GO terms related to a total of 9,132 genes (*i.e.*, 63% of the genes had associated GO terms), which was used as the background for GO enrichment. Analysis was performed using the enricher function in clusterProfiler v4.8.2 (Yu et al., 2012), using a minimum gene size of 10 and a maximum gene size of 500, and an FDR value ≤ 0.05.

Finally, we identified hub genes for the modules of interest, which correspond to highly connected nodes that can be representative of that module's main function (Lanfelder and Horvath, 2008). We first calculated intramodular connectivity (kIM) for genes within each module in the Emperor penguin network with the *intramodularConnectivity.fromExpr* function, using the biweight midcorrelation (*bicor* function) (Langfelder & Horvath, 2012). We then determined hub genes by selecting nodes with kIMs equal to or higher than the 90th quantile of the module's kIM distribution.

2.5.3 Analysis of differentially expressed genes (DEGs)

To identify the patterns and biological functions of differentially expressed genes (DEGs) across the five tissues, we performed a standard analysis of differential gene expression using DESeq2 (Love et al., 2014). We specified '~ Group' as the negative binomial GLM formula, where 'Group' was defined as 'Tissue+Species'. Contrasts were performed between the tissue of each species using the Emperor penguin as the baseline. An FDR threshold < 0.01 and a log2foldchange > 2 or < -2 was used to determine significant DEGs, where

Emperor penguin under-expressed genes (and thus King penguin over-expressed genes) are indicated by a positive log2foldchange and Emperor penguin over-expressed genes (thus King penguin under-expressed genes) are indicated by a negative log2foldchange. Volcano plots were plotted using EnhancedVolcano (Blighe et al., 2018). To limit our search space for most likely gene candidates, we specifically explored the gene annotations of the top ten under-expressed or over-expressed DEGs (ordered by adjusted p-value) for each tissue in the Emperor penguin.

3. Results

3.1 *De novo* transcriptomes of the Emperor penguin and King penguin

Full assembly and quality statistics of the *de novo* transcriptomes can be found in Table S3. We generated >105 million clean paired-end reads for the Emperor penguin. The final assembled transcriptome contained 106,060 contigs, with an average length of 1,047 bp, an N50 of 2,429 bp. In the King penguin, we generated >92.5 million clean paired-end reads. The final assembled transcriptome contained 80,605 contigs, with an average length of 1,291 bp, an N50 of 2,511 bp.

Assessment of both transcriptomes revealed a high assembly quality in both species. Alignment of the reads back to each species' respective transcriptomes showed that 82.3% of the reads aligned to the Emperor penguin transcriptome and 78.6% of reads aligned to the King penguin transcriptome. The Emperor penguin transcriptome had an E90N50 value of 3,408 bp (corresponding to 38,973 transcripts; Figure S3); and the number of transcripts expressed at >1 TPM was 89,898. The King penguin transcriptome had an E90N50 value of 3,398 bp (corresponding to 24,981 transcripts; Fig. S3); the number of transcripts expressed >1 TPM was 66,467. BUSCO analysis of both transcriptomes also revealed high completeness: 86.3% in the Emperor penguin and 84.3% in the King penguin.

In functional annotation of the Emperor penguin, 63,310 transcripts were annotated using Trinotate, of which 56,279 annotated to genes using BLASTX (53%), and 37,202 were annotated to genes using BLASTP (35%). In the King penguin transcriptome, we identified 62,518 annotated transcripts, of which 55,239 were annotated to genes using BLASTX (69%), and 38,317 were annotated to genes using BLASTP (48%). Transcriptome annotations are available on GitHub (Paris et al., 2023).

3.2 High conservation of gene expression across tissues between the Emperor and King penguin

We sampled ten biological replicates from five tissues of Emperor and King penguin chicks and used 3' QuantSeq to describe the patterns of gene expression for each tissue. Across the independent samples, we obtained an average of 6,181,711 (SEM ± 184,196) clean reads for the Emperor penguin and an average of 8,439,985 (SEM ± 315,902) clean reads for the King

penguin (Table S4). Assessment of the counts showed good consistency across replicates and tissues (Figure S4). One biological replicate of the brain from the Emperor penguin (EB04) was removed due to a low number of recovered reads (Table S4).

Evaluation of the ordination of the samples via PCA revealed high tissue-specific clustering of the biological replicates in both the genome-mapped data (Figure S5) and transcriptome-mapped data (Figure 1A & 1B). In the transcriptome-mapped data, the samples clustered by tissue in both species, with both PC1 and PC2 explaining a similar proportion of the variance. PC1 primarily separated all tissues, except for skin and brain, which were separated by PC2. In the Emperor penguin, the muscle was more different on both axes. Separation of the skin tissue was less apparent in the Emperor penguin data, due to two replicates which deviated from the tissue's centroid. Further inspection of these outlier samples identified no artifactual reasons for removal of these replicates; therefore, they were retained in downstream analyses.

Overall, assessment of the tissue-enhanced and -inhibited genes showed very similar patterns between the two species (Figure S6; Table S5), with brain and skin tissues showing high tissue-specificity in both species (Fig. 1C & 1D). Kidney-enhanced transcripts were shared mostly with the liver, and the same vice versa in the liver-enhanced transcripts. Muscle-enhanced transcripts showed some shared expression with the skin and the brain, whereas skin-enhanced transcripts were not shared in the muscle, but more in the kidney. Despite the overall highly shared landscape of tissue expression in both species, the numbers only reflect general patterns of tissue regulation.

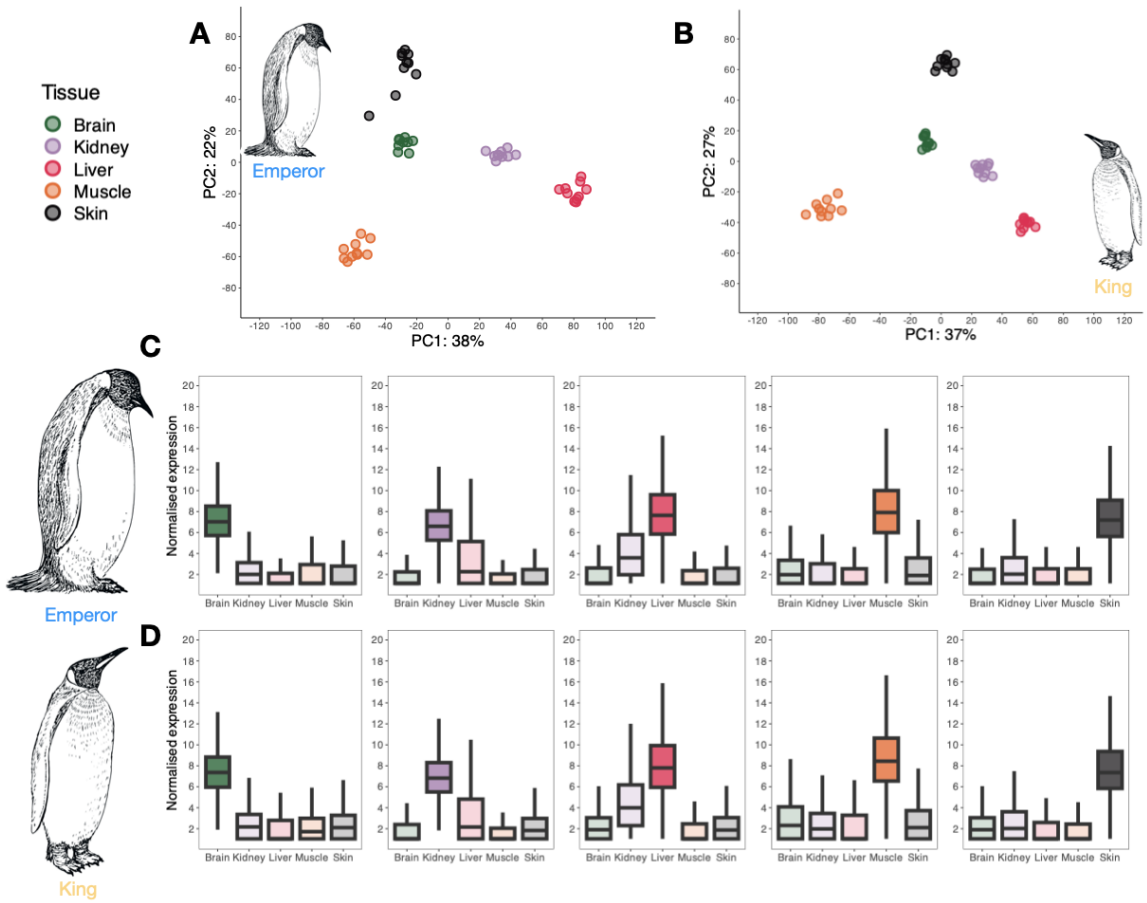

Figure 1. Tissue-specific patterns of gene expression in the Emperor and the King penguin. (**A, B**) Principal Components Analysis (PCA) of the normalised expression of tissues in the (**A**) Emperor penguin or (**B**) King penguin. In both PCAs, samples are coloured by tissue as shown in the legend: brain (green); kidney (purple); liver (pink); muscle (orange); skin (black). (**C, D**) Variance Stabilising Transformation (VST) normalised expression counts of the tissue-enhanced genes in the (**C**) Emperor penguin or (**D**) King penguin.

3.3 Identifying unique tissue-specific genes and biological processes in the Emperor penguin

Given the high similarity of the patterns of tissue-enhancement and -inhibition between the species, we next aimed at identifying the tissue-specific genes that were unique to the Emperor penguin and the King penguin. For comparative purposes, we used only those transcripts which could be annotated (hereafter referred to as “genes”; see Table S6 for full details). Looking at all enhanced and inhibited genes (Venn diagrams; Figure 2), the brain showed the highest number of shared genes (45%; Fig. 2A), with the liver (32%, Fig. 2C) and skin (32%, Fig. 2E) showing the fewest number of shared genes. Inspecting the number of tissue-enhanced genes (TEGs) unique to each species, the brain and liver showed a higher number which were unique to the Emperor penguin. In the brain, the proportion of unique TEGs was similar between the species (Fig. 2A), while the King penguin showed a higher number of enriched GO terms (32 compared to 4 in the Emperor penguin; see Table S7 for a full list of significant GO terms for each tissue). In the liver, although the King penguin had a

higher proportion of unique TEGs, these were associated with only four GO terms. In contrast, Emperor penguin liver TEGs were associated with 67 GO terms (Fig. 2C), related to metabolism, in particular lipid and glucose metabolism, energy production, and food intake, including digestion, regulation of feeding behaviour, and response to starvation (Table S7). The kidney and skin showed a lower total number of unique genes in the Emperor penguin, the proportion of which were tissue-enhanced were higher in the Emperor penguin kidney, but lower in the skin (Fig 2B & 2E). GO terms enriched in the kidney appeared to be unrelated to adaptation in the Emperor penguin. Although the skin showed a lower proportion of TEGs unique to the Emperor penguin, these were associated with seven GO terms (Fig. 2E), with potential relevance to adaptation, including epidermis development, canonical Wnt signalling pathway involved in positive regulation of epithelial to mesenchymal transition, and positive regulation of heparan sulphate proteoglycan biosynthetic process. Finally, the muscle showed the lowest number of total genes unique to the Emperor penguin (20%; Fig. 2D), but a higher proportion of these were tissue-enhanced (0.51) in comparison to the King penguin (0.43). GO analysis of these TEGs identified four enriched terms in the Emperor penguin, potentially related with adaptation, including muscle cell fate commitment, and positive regulation of skeletal muscle fibre development, whereas no terms were associated with the King penguin TEG set (Fig. 2D).

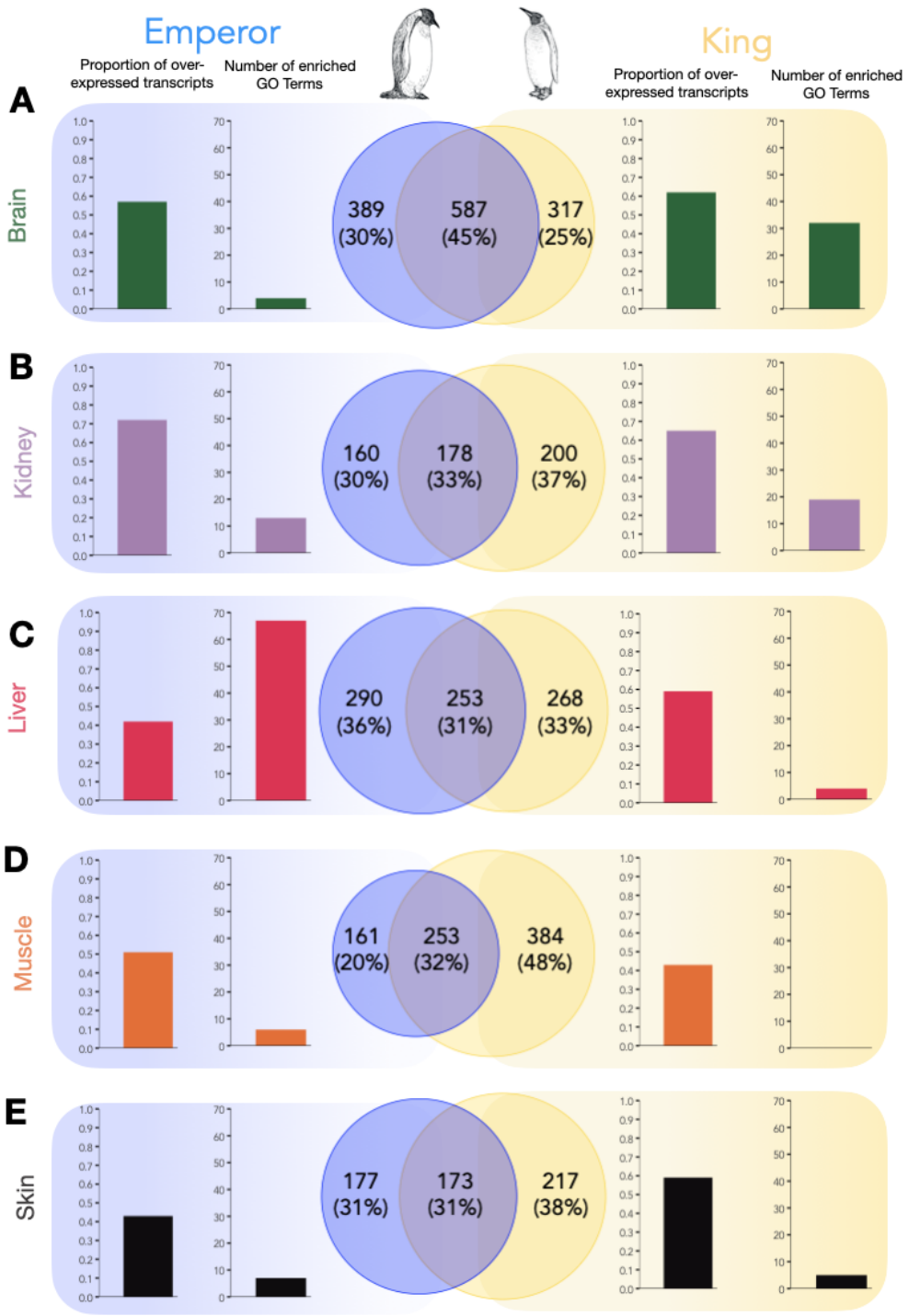

Figure 2. Quantification of unique tissue-specific genes in the Emperor penguin and King penguin. For each tissue (**A**: brain; **B**: kidney; **C**: liver; **D**: muscle; **E**: skin) the Venn diagrams represent the total number of unique genes (both tissue-enhanced and tissue-inhibited) in the Emperor penguin (in blue, left) and the King penguin (in yellow, right). Intersect reflects the number of shared tissue-enhanced genes. Bar plots show the proportion of unique tissue-enhanced genes (TEGs) for each species, and the number of enriched GO BP terms related to each species' set of TEGs.

3.4 Identifying regulatory changes in the Emperor penguin

We next investigated differences in the regulatory landscape of gene expression by constructing weighted co-expression networks in WGCNA. The Emperor penguin network was characterised by 1943 genes assigned to 12 modules (*i.e.*, gene clusters, defined by colour names) and 756 genes that were not assigned to any module ("grey module"), while the King penguin network contained 2042 genes assigned to 15 modules and 657 genes not assigned to any module (Figure 3A, Table S8). For further analyses, we focus on the relationship between Emperor penguin modules with the different tissues and their preservation in the King penguin network.

In accordance with the strong tissue-specificity enhancement observed at the transcript-level (Fig. 1), we also observed an association between the module eigengenes (ME) and the tissues in both species (Fig. 3B). More specifically, three Emperor penguin modules had moderate ($0.5 > cor < 0.7$) to high positive correlations ($cor \geq 0.7$) with the brain (turquoise, red, and brown). Four modules were correlated with the liver (green, black, blue, and pink), five modules with the muscle (purple, yellow, tan, pink, and brown), and two modules with the skin (magenta and greenyellow) (Figure S7). No modules were significantly correlated with the kidney.

Computing preservation statistics on the 12 Emperor penguin modules, we identified six modules as weakly preserved in the King penguin: green, pink, tan, yellow, purple, and turquoise. Overall, the purple module (associated with the muscle) was the least preserved (Table S9, Figure S8). In particular, the statistics that explained this module's low preservation were the mean Maximum Adjacency Ratio (*meanMAR = 0.149*) and the Proportion of Variance Explained (*propVarExpl = 0.146*) by the ME (Fig. 3C, Table S10). Low *meanMAR* values indicate that genes from an Emperor penguin module have weak correlations in the King penguin network, even if those genes have a high number of connections (*i.e.*, high density). *propVarExpl* is a density statistic that measures how tightly correlated are genes from a module in the test dataset based on the module's eigengene (*i.e.*, expression variance in that module) (Langfelder et al., 2011). Two other muscle modules, yellow and tan, the muscle-liver pink module, and the liver green module also showed low values of *meanMAR* statistics (Fig. 3C, Table S10). In accordance with low *meanMAR* values, we also detected a tendency towards lower intramodular connectivity (kIM) values (*i.e.*, weaker connections) among genes of the three muscle modules, purple, yellow, and tan, in the King penguin network in comparison to the Emperor penguin network (kIM distribution shifted to the left in the King penguin; Fig. 3D; further details on kIM in Langfelder & Horvath, 2008). Another module that showed signals of weak preservation in the King penguin dataset was the brain-related turquoise module, with a *propVarExpl* = 0.200 (Fig. 3C, Table S10).

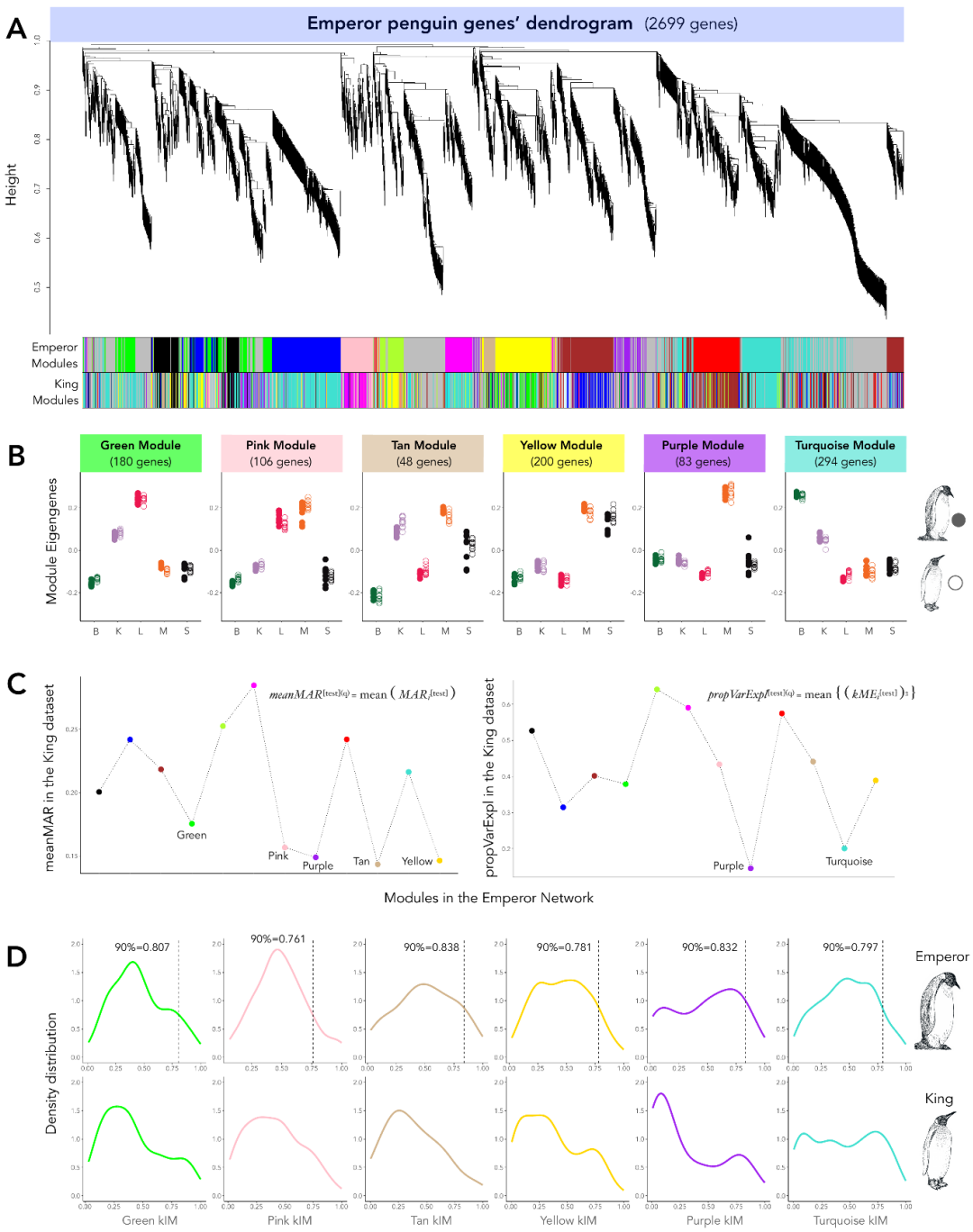

Figure 3. Dendrogram and modules of interest in the Emperor penguin co-expression network. **(A)** Dendrogram of genes clustered based on topological overlap between nodes (*i.e.*, genes), and their assigned modules in the Emperor penguin network (top colours). King penguin modules defined in the King penguin network are represented in the bottom colours to illustrate module assignment differences between the two networks, while all other plots (B), (C) and (D) are based on the Emperor penguin network modules. **(B)** Module eigengenes (ME, corresponding to the PC1 of the module's expression profile) of weakly preserved Emperor penguin modules in the King penguin network according to the *Z* permutation and *medianRank* statistics (Fig. S8 & Table S9), where B stands for brain, K for kidney, L for liver, M for muscle, and S for skin samples. Filled and empty dots represent Emperor penguin and King penguin samples, respectively. **(C)** Main summary statistics that indicate the weak preservation of purple, yellow, tan, pink, turquoise, and green Emperor penguin modules in the

King penguin network. In the left panel, the mean Maximum Adjacency Ratio (*meanMAR*) statistics, in which low *meanMAR* indicates modules composed of nodes with weak connections (*i.e.*, co-expression) with neighbour nodes in the King penguin dataset. In the right panel, the Proportion of Variance Explained by the module eigengenes (*propVarExpl*), in which low *propVarExpl* indicates low module density in the King penguin dataset, as correlation between gene expression patterns are lower. **(D)** kIM densities of genes of the least preserved modules (green, pink, tan, yellow, purple, and turquoise) in Emperor penguin (top) and King penguin (bottom) networks. Dashed vertical lines in the Emperor penguin plots indicate the 90th quantile of kIM distribution threshold used to determine hub genes (Table S12).

To investigate the biological meaning of the six candidate Emperor penguin modules: purple (muscle); yellow (muscle); tan (muscle); pink (muscle & liver); green (liver); turquoise (brain), we performed GO term enrichment analysis on all genes identified within each module (see Table S11 for full results). The purple module was significantly enriched for 11 GO terms related to muscle development and organisation, as well as heart activity regulation. The two other muscle modules, tan and yellow, were significantly enriched for 7 and 11 GO terms, respectively. GO terms of both modules related to embryonic cell organisation and differentiation, while the yellow module was also enriched for two GO terms related to stress response and hypoxia. The green liver module had one enhanced GO term related to blood coagulation. The pink (muscle and liver) module had one enhanced GO term related to fatty acid beta-oxidation. The turquoise brain module had six enriched GO terms related to neural cell formation and function.

An additional method to assess the biological meaning of module function is through the detection of hub genes, which are highly connected genes within a module (*i.e.*, nodes with high kIM values), usually representative of the module's main regulatory role (Langfelder & Horvath, 2008). By selecting genes using the upper 90th quantile of the module's kIM distribution for the Emperor penguin (Fig. 3D), we detected nine hub genes in the purple muscle module, 20 genes in the yellow, and five genes in the tan module. The pink and green modules contained 11 and 18 hub genes, respectively, and the turquoise brain module has 30 hub genes (Table S12).

3.5 Differentially expressed genes between the Emperor penguin and the King penguin

Finally, using the transcript data mapped to the Emperor penguin genome, we sought to identify the patterns and potential function of differentially expressed genes (DEGs) between the species across the five tissues (Figure 4). We found that the muscle showed more than double the number of DEGs (n=786), where the majority (n=598, 78%) were over-expressed in the Emperor penguin (Table S13). This was followed by the skin (n=300; 63% over-expressed, 37% under-expressed), liver (n=287; 46% over-expressed, 54% under-expressed), kidney (n=183; 74% over-expressed, 26% under-expressed), and finally the brain (n=77, 35% over-expressed, 65% under-expressed). We specifically explored the top ten over-expressed or under-expressed genes in each tissue (Table S14), and performed an extensive literature

search on these candidates, considering genes related more intimately to the biology of the Emperor penguin in the discussion. Assessment of the top candidate genes revealed that some DEGs were identified as consistently over-expressed (six genes) or under-expressed (3 genes) in more than one tissue (Table 1).

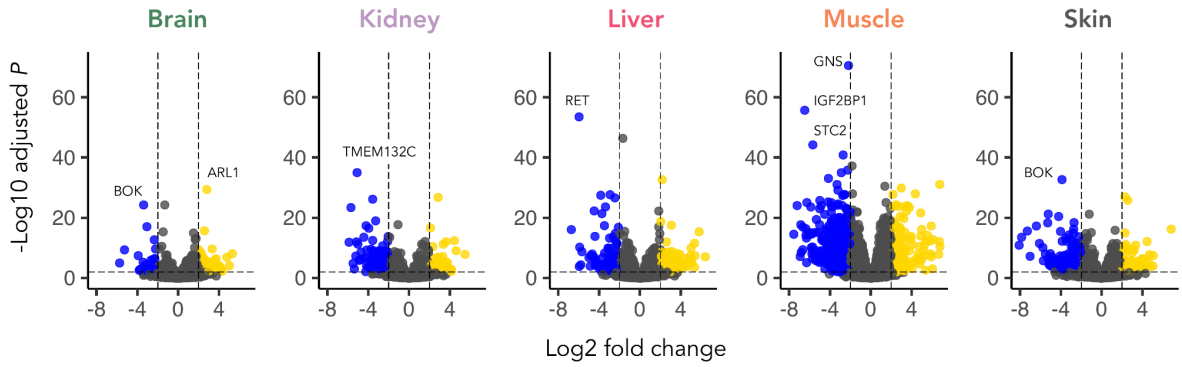

Figure 4: Volcano plots of the 10,797 genes included in the differential expression analyses between Emperor penguin and King penguin per tissue. Coloured dots correspond to DEGs with *padj* > 0.01 and $\log_2$ fold changes < -2 (blue) and > 2 (yellow), meaning their upregulation in the Emperor penguin and King penguin, respectively. The gene IDs of highly differentiated genes are included.

Table 1. Differentially expressed genes (DEGs) identified as over- or under-expressed in more than one tissue in the Emperor penguin.

Gene Symbol	Tissues	Expression in Emperor penguin
BOK	brain, skin, kidney	Over-expressed
LOC103895152	brain, kidney, liver	Over-expressed
LARP1	brain, liver	Over-expressed
ACP6	brain, kidney	Over-expressed
TEX33	brain, kidney, liver	Over-expressed
MLST8	kidney, liver	Over-expressed
STC2	liver, muscle	Over-expressed
ARL1	brain, kidney, muscle, skin	Under-expressed
PPP1R37	brain, kidney, skin	Under-expressed
GOLPH3L	brain, kidney	Under-expressed

Discussion

By performing a comparative multi-tissue profiling of the Emperor penguin and the King penguin, we evaluated the role of gene expression in adaptation to the extreme conditions of Antarctica experienced by the Emperor penguin. We hypothesised that if gene regulation is important, the signal of gene expression divergence should be more related to the specific phenotype of the Emperor penguin, rather than to broader biological processes important for both species. We emphasise that due to sampling restrictions in the wild, our analyses were performed on tissues sampled from chicks, but that our interpretation concerns gene expression related to hardcoded adaptive differences between the species, which should not only be related to later developmental stages. We generated the first high-quality reference transcriptomes for both species. Enrichment analysis on the annotated tissue-enhanced transcripts unique to the Emperor penguin identified a suite of relevant biological processes related to the metabolic demands imposed by the cold, and fasting, in particular in the liver and muscle. We next assessed the regulatory landscapes of both species, classifying six Emperor penguin co-expressed modules associated with the muscle, liver and brain which were weakly preserved in the King penguin. Through analysis of differential gene expression between the two species, we found that the muscle showed more than double the number of differentially expressed genes compared to all other tissues. By exploring the genes and processes identified across the analyses, we are able to pinpoint the tissues and potential candidate genes responsible for gene-expression mediated adaptive plasticity in the Emperor penguin.

Brain

As a highly specialised and complex tissue, the brain often shows unique patterns of gene expression in comparative studies (Bentz et al., 2019; GTEx Consortium, 2015; Qi et al., 2019) and our analysis of brain-enhanced transcripts also highlighted this tissue as particularly unique (Fig. 1C & D). We also observed the lowest annotation rate for the unique brain-enhanced transcripts (Table S6), which is expected given the high specificity of brain genes and an obvious bias in annotation towards model species (Sjöstedt et al., 2020). When comparing gene expression patterns between the species, the brain had the lowest signature of differential gene expression. Yet at the regulatory level, a lower degree of conservation was observed, as the largest co-expression module in the Emperor penguin (turquoise, n=294) was related to the brain and was weakly preserved in the King penguin. This pattern indicates that, despite the high correspondence of the over-expressed and under-expressed sets of genes in both species, the regulatory pathways through which such genes interact in the brain are likely different. However, interpreting such regulatory differentiation and its biological relevance to the Emperor penguin ecological (cold, absence of daylight) and physiological (metabolic balance during long fast periods) adaptation is challenging, as the majority of enriched GO categories in our analyses appeared to be primarily functional (*i.e.*, involved in cell-cell signalling, cell adhesion, and synapse, axon, and neuron processes).

Still, amongst the turquoise module hub genes and the most significant over-expressed genes, we identified a set of potentially relevant candidates (Table S12 & S14). Related to cold adaptation we identified two genes: SLC6A1, which encodes the GAT1-GABA transporter and has been previously implicated in adaptive cold-stress responses in *Anolis* lizards (Campbell-Staton et al., 2017); and ITPR1, a neuronal intracellular calcium release regulator critical to nociception and pain behaviour (Petrenko et al., 2003), which in particular, has been shown to be regulated under repeated cold stress in rats (Kozaki et al., 2015; Wakatsuki et al., 2021). We also identified genes related to nutrient regulation and metabolism. The most significantly over-expressed gene in the brain, BOK, was also the top significant gene in the skin, and was also highly over-expressed in the kidney (Table 1). BOK is one of the main mitochondrial apoptosis regulators, which is activated in response to stress stimuli, such as DNA damage, oxidative stress, aberrant calcium fluxes, and nutrient deprivation (Lopez & Tait, 2015). The known role of this gene in regulating fasting in humans and chickens is suggestive of a similar mechanism in the Emperor penguin (Giménez-Cassina & Danial, 2015). LARP1, a key regulator of the mTOR pathway, was the second most over-expressed gene in the brain, and the fifth most over-expressed gene in the liver. The mTOR pathway is regulated in response to growth signals and nutrient availability (Kim et al., 2002) and is involved in metabolic stress adaptation (Wu & Storey, 2021). Interestingly, under nutritional limitations, mTOR acts as a metabolic switch to lower global metabolism (Fuentes et al., 2021), suggesting this gene may be important in the regulation of metabolism under fasting conditions. ACP6 (also highly over-expressed in the kidney) regulates mitochondrial lipid biosynthesis by balancing lipid composition within the cell (Li et al., 2013). We also identified MTNR1A as differentially expressed (although not within the top candidates), which mediates melatonin effects on circadian rhythm and reproductive alterations affected by day length (Fishman & Tauber, 2023), which could be relevant as Emperor penguin reproduction occurs during the almost constant darkness of austral winter (Miché et al., 1991).

Kidney

Due to the kidney's role in osmoregulation and renal function, we hypothesised that this tissue might reflect processes related to the high metabolic demands of the Emperor penguin. Indeed, we observed that kidney-enhanced transcripts shared some expression patterns with the liver, potentially reflecting a common landscape of metabolism (especially glucose), which has been previously observed in birds (Braun, 2015; Sparr et al., 2010; Tinker et al., 1984). However, aside from the identification of an enriched pathway involved in the regulation of insulin-like growth factor receptor signalling (Table S7), which is directly implicated in renal function under fasting conditions (Feld & Hirschberg, 1996; Hirschberg & Kopple, 1989), we observed few other biological processes related specifically to Emperor penguin adaptation. Additionally, no co-expressed modules were significantly correlated with this tissue, which also showed the second lowest number of DEGs. However, amongst the over-expressed genes, we did identify BOK and APC6 (discussed above). RBP4, the third most over-expressed gene, encodes for a specific retinol carrier in the blood, transporting

retinoids (vitamin A and its derivatives) to target tissues, such as adipose tissue (Steinhoff et al., 2022). Previous reports in mice revealed that retinol transport proteins are potent regulators for cold-induced thermogenic responses and cold adaptation by promoting expression of marker genes in the adipocytes (Fenzl et al., 2020; Ribot et al., 2004). Finally, no gene candidates overlapped amongst our analyses for the kidney (Table S15), and the overall concerted signal of the role of this tissue in Emperor penguin adaptation was low.

Skin

We reasoned that the skin would show a gene expression profile related to thermal insulation and the development of feathers, as the Emperor penguin's thick skin and morphologically specialised plumage is one of the keys to survival in Antarctica (Williams et al., 2015). These specialised dermic structures can provide 80–90% of insulation requirements (Le Maho, 1977b; Le Maho et al., 1976), enabling them to maintain a core body temperature of 38°C (Ponganis et al., 2003). In particular, such adaptations should be observed in the early life stages, as Emperor penguin chicks are covered in a unique down that confers a thermoregulatory advantage (Taylor, 1986). Aside from the yellow muscle module (which also showed a low degree of correlation with the skin; Figure S7), we did not find any co-expression modules uniquely preserved in the Emperor penguin, and overlap amongst analyses was low (Table S15). However, in the analysis of Emperor penguin unique skin-enhanced TEGs, we identified three enriched GO term processes which could be involved in the development of feathers, including epidermis development (Yu et al., 2004), canonical Wnt signalling pathway (involved in positive regulation of epithelial-to-mesenchymal transition; Heller & Fuchs, 2015), and heparan sulphate proteoglycan biosynthetic process (related to hair follicle and sebaceous gland morphogenesis; Coulson-Thomas et al., 2014). Amongst the most highly over-expressed genes, we identified BOK (discussed above), ANO1, which acts as an excitatory heat-activated channel in mammalian thermosensation (Cho et al., 2012; Vriens et al., 2014), a gene (LOC103893312) encoding an adipocyte fatty acid-binding protein, LPL, a key triglyceride metabolism enzyme, involved in cold-stress responses in birds (Bénistant et al., 1998; Radomski & Orme, 1971), and PLIN1, a lipid droplet coat protein, which affects body weight and fat deposition (Bickel et al., 2009). ALPK3, was identified in all analyses (Table S15), and although primarily implicated cardiomyopathy, this gene has been identified as a plasticity candidate in a gene expression analysis of temperature responses in stickleback (Metzger & Schulte, 2018). The role of these pathways and genes in feather development, thermosensation, and energy storage are distinctly relatable to the Emperor penguin’s ecology. However, overall, the skin had a lower signal compared to the muscle and liver, which may be due to its more highly shared thermoregulatory function in both Emperor and King penguins (Lewden et al., 2017), especially in chicks (Duchamp et al., 2002).

Muscle

Since muscle contraction is coupled to heat production, the muscle is the primary thermogenic organ in most vertebrates (Periasamy et al., 2017). We found that the unique

expression profile in this tissue was particularly conspicuous, encompassing a high proportion of tissue-enhanced transcripts related to enriched GO processes relevant to cold adaptation (Fig. 2), four of the six significantly divergent modules in the co-expression analysis (Fig. 3), and the largest fraction of differentially expressed genes (Fig. 4; 76% of which were over-expressed in the Emperor penguin). The muscle was also the only tissue showing a high amount of overlapping candidate genes across our analyses (Table S15). Although the muscle is a highly specialised tissue, the signatures of gene expression were not limited to a narrow set of genes or processes involved only in the structural organisation of muscle fibres. Instead, our findings are consistent with the crucial role played by the muscle in temperature homeostasis and whole body energy metabolism (Swanson et al., 2022).

Skeletal muscle produces heat primarily through shivering thermogenesis (Periasamy et al., 2017), which involves rapid, repeated muscle contractions (Nakamura & Morrison, 2011). Accordingly, we identified muscle contraction and striated muscle contraction as enriched GO processes in the least preserved co-expression module (purple) and in uniquely enhanced genes in the Emperor penguin. Although these could also be related to locomotion, locomotor activity in chicks is very low as they are brooded on the adults' feet, and activity only increases prior to fledging (Corbel et al., 2009). Moreover, relative to total body mass, the skeletal muscle of birds is commonly much larger than that of reptiles and mammals, and it has been hypothesised that this enlargement allows for more effective heat generation, especially in breast and thigh muscles (Newman, 2011; Rowland et al., 2015). We detected positive regulation of skeletal muscle fibre development as an enriched GO process in the analysis of unique genes and skeletal muscle tissue development was identified as the most significantly enhanced process in the purple module. Moreover, the most central gene in the purple module was VWDE (also present as an Emperor penguin unique TEG), which in humans, is associated with breast hypertrophy (Rappaport et al., 2013). Amongst the most highly over-expressed genes, we also identified FN1, a glycoprotein that links fibrillar matrix tissue, providing strength and elasticity to muscle fibre (Smith et al., 2013), and METRNL, which is induced in skeletal muscle upon exercise and during exposure to cold (Bae et al., 2018; Rao et al., 2014). In mouse models, METRNL increased *in vivo* in exercised mice, suggesting that METRNL is secreted during repeated muscle contraction, and injected METRNL improved glucose tolerance in mice with high-fat-diet-induced obesity or diabetes (Lee et al., 2020). We also identified the gene EYA1 as overlapping in all analyses. EYA1 has been shown to be involved in the metabolic and contractile specialisation of mature muscle fibres (Grifone et al., 2007). EYA1 proteins accumulate preferentially in the nuclei of fast-twitch glycolytic muscles (Grifone et al., 2004), which have been shown to play a prominent role under acute cold exposure in rats (5°C; Wang et al., 2003).

Whilst shivering is considered to be the dominant mechanism of heat production in birds (Bicudo et al., 2001), recent empirical evidence also argues for the role of non-shivering thermogenesis (NST; Teulier et al., 2010). In mammals, NST is regulated by the activity of uncoupling protein 1 (UCP1) in brown adipose tissue (Klingenspor, 2003). Although birds lack

brown adipose tissue and mammalian UCP1 (Mezentseva et al., 2008), evidence of a homologous functional avian UCP accompanied by empirical evidence of whole-body metabolic heat production unrelated to shivering suggests NST represents a plausible additional mechanism of thermogenesis in birds (Hohtola, 2002; Raimbault et al., 2001; Teulier et al., 2014). Although Emperor penguins lack empirical evidence of NST, data from the King penguin suggests NST occurs in via concerted mechanisms in the skeletal muscle (Duchamp et al., 1991; Duchamp & Barré, 1993; Talbot et al., 2004; Teulier et al., 2010). The first mechanism includes increased activity of avian UCP, which is dependent on superoxide, a reactive oxygen species (ROS). Compared to other Antarctic birds, Emperor penguins exhibit higher ROS scavenging capacity, suggesting they are naturally exposed to higher basal prooxidant pressures (Corsolini et al., 2001). Related to this, we identified two enriched GO processes in the yellow (muscle) module related to the cellular response to ROS. Moreover, the negative regulation of S-nitrosylation, which is a selective protein modification mediated by ROS (Stomberski et al., 2019) was identified in the purple module, and has been previously implicated in mammalian NST (Sebag et al., 2021). Amongst the top over-expressed genes in the Emperor penguin, we also identified IGF2BP1, an insulin-like growth factor which stabilises mRNA molecules that are recruited to stress granules under oxidative stress and heat shock (Bley et al., 2015), which is specifically induced in chickens under high-fat diets (Chen et al., 2019). The second potential mechanism of NST is increased activity of the adenine nucleotide translocase, which is dependent on the oxidation of fatty acids. The only enriched GO process in the pink module (related to both the muscle and the liver) was fatty acid beta-oxidation. Whilst these pathways are indicative of a potential role of NST in Emperor penguin gene expression adaptation to the cold, such responses should be confirmed by physiology studies.

Adipose tissue is also a fundamental regulator of energy homeostasis (Zhuo et al., 2015), and has an important role in metabolic energy storage (Choe et al., 2016). In Emperor penguins, fat stored in adipose tissue is by far the major energy reservoir (Groscolas & Robin, 2001), with body fat at the beginning of the breeding fast representing approximately 30% of the body mass and 80% of body energy (Groscolas, 1990). Our decision to not sample this tissue was in part, due to evidence of the higher importance of skeletal muscle for NST in birds, in addition to the low nucleic acid content in adipocytes (Cirera, 2013; Sinitsky et al., 2018). However, we still identified recurrent signals of genes related to adipogenesis in our analyses, including several significant genes identified as adipocyte fatty acid-binding proteins (Paris et al., 2023), and two genes (MEOX1 and POSTN), which were uncovered as overlapping in all three analyses of the muscle. The homeobox protein MEOX1 is a mesodermal transcription factor involved in somitogenesis and the commitment of cells to the skeletal muscle lineage (Petropoulos et al., 2004; Wu et al., 2018). MEOX1 expressing progenitors in the somite revealed that both brown and white adipocytes arise from the somitic mesoderm (Shamsi et al., 2021). POSTN (also identified as a hub gene in the yellow module) is a secreted extracellular matrix protein that functions in tissue development and regeneration, and is produced and secreted by adipose tissue. A transcriptomic analysis of

porcine adipocytes showed that POSTN was a crucial candidate gene associated with adipogenesis during the differentiation of intramuscular adipocytes (Mo et al., 2017). In mice, the adaptation of adipose tissue to high-fat diet feeding is impaired in animals with systemic ablation of POSTN, suggesting that a loss of periostin attenuates lipid metabolism in adipose tissue (Graja et al., 2018).

Liver

With the liver's key role in digestion and metabolism, specifically in regulating the production, storage, and release of lipids, carbohydrates and proteins (Zaefarian et al., 2019), we hypothesised gene expression differences in this tissue to be related to the strong metabolic demands typified by the life cycle of the Emperor penguin. In line with this, the liver showed marked differences between the two species, associating to more than 60 enriched GO terms in the analysis of unique TEGs, showing an association to two co-expression modules (green and pink - also correlated to muscle tissue), which were weakly conserved in the King penguin, and a high number of differentially expressed genes (n=287). Fasting in the Emperor penguin is characterised in three phases. In particular, Phase II is defined by a long period of protein sparing and preferential mobilisation of fat stores, where proteins account for 4% of energy reserves, and lipids for the remaining 96%, followed by Phase III which is defined as a period of increased net protein catabolism (Groscolas & Robin, 2001; Robin et al., 1988). Such fasting periods are carefully controlled by metabolic and endocrine shifts, which we can assume are hardcoded early in life. We observed a striking signal of processes directly relatable to this biology in the analysis of unique liver TEGs, including GO terms enriched for digestion, regulation of feeding behaviour, adult feeding behaviour, intestinal absorption, regulation of peptide hormone, cellular response to parathyroid hormone stimulus, and response to starvation. In addition, we identified ten processes related to lipid metabolism, 12 terms related to glucose, glycolysis, and gluconeogenesis, and four terms related to energy production, including NADH regeneration and response to cAMP. We also uncovered the enrichment of fatty acid beta-oxidation in the pink co-expression module (also correlated with the muscle). Moreover, in fasting birds, including Emperor penguins, plasma uric acid concentrations are known to reflect the intensity of protein catabolism (Cherel et al., 1988; Robin et al., 1998), and we identified four enriched GO terms related to uric acid production, including the urea cycle and urate biosynthesis. Additionally, processes involved in vitamin D and retinoic acid were identified, which are also involved in mTOR signalling (Lisse & Hewison, 2011). Overall, this strong signature of highly relevant biological processes enriched uniquely in the liver of the Emperor penguin highlights the important role of this organ for crucial metabolic processes later in life. Importantly, we detected these pathways as already under potentially adaptive gene regulation in chicks.

Interestingly, in analysis of the liver-specific co-expression module (green) the only enriched GO term was blood coagulation, and this was also identified in analysis of unique tissue-enhanced genes, providing additional evidence on the importance of this process. The liver plays a key role in blood coagulation, where it synthesises the majority of proteins involved in

fibrinolysis (Mitra & Metcalf, 2012). In humans, metabolic fatty liver disease is associated with heightened blood coagulation (Tripodi et al., 2022; Valenti et al., 2022), indicating that the high rate of lipid storage and subsequent metabolism likely affects the balance of blood coagulation in Emperor penguins. Previous studies have identified blood coagulation genes as under positive selection in *Aptenodytes* penguins (Cole et al., 2022), but the finding of particular enrichment of this process in Emperor penguins in this study, suggests disparate mechanisms of gene regulation between the two species. Finally, in analysis of the differentially expressed genes, we identified a suite of candidates involved in lipid metabolism, and glucose and insulin regulation. RET was the most highly over-expressed gene in the liver, which is a well-known oncogene in humans (Jhiang, 2000), and has been linked to lipid accumulation in humans (Söhle et al., 2012) and chickens (Sun et al., 2013). LARP1 (also identified in the brain) was also highly over-expressed, and as mentioned above, is a key regulator of the mTOR pathway. Related to this, we also identified MLST8 (also highly over-expressed in the kidney), which is another key regulator of the mTOR pathway, essential for growth signalling and metabolism (Wullschleger et al., 2006). STC2, a secreted glycoprotein hormone, was identified in all three analyses (Table S15), and is involved in the regulation of insulin-like growth factors and glucose (Sarapio et al., 2019). In obese mice, overexpression of STC2 significantly attenuated fatty liver and hypertriglyceridemia (Zhao et al., 2018). Overall, the strong signature of the liver, together with the muscle, suggests that these two tissues are most important in gene expression adaptation in Emperor penguins.

Conclusions

When a population colonises a new environment, gene expression becomes crucial in guaranteeing persistence, mediating phenotypic plasticity, and contributing to the early phases of adaptive divergence (Pavey et al., 2010). Genetic divergence in adaptive traits over time eventually leads to reproductive isolation between populations (Fay & Wittkopp, 2008; Pavey et al., 2010). Unlike changes in coding genes, changes in gene expression may speed up adaptive evolution, especially under strong selection pressures over short timescales (Brauer et al., 2017; Jones et al., 2012; Uusi-Heikkilä et al., 2017). More explicitly, changes in gene expression are expected to respond quicker than mutations in coding sequences when a population colonises a novel environment (Josephs, 2021). In fact, only gene expression effects can be moulded to enhance or inhibit the role of genes in a particular tissue(s). Given recent evidence that a large fraction of genes take part in multiple, if not all, cellular pathways (*i.e.*, the omnigenic model; Boyle et al., 2017), novel protein mutations which can confer an advantage under specific environmental conditions while not disrupting any of the other protein functions are expected to be rare (*i.e.*, slowly appearing). Under this perspective, regulatory changes in gene expression could match, or likely surpass, standing coding sequence diversity as the first adaptive tool to quickly respond to fast environmental change (Burton et al., 2022). However, quantifying gene expression differences and relating these to divergent ecological adaptations is a complex task and describes the interrogation of only a single aspect of the extremely complex genotype-to-phenotype association. This study therefore represents a first contribution to understanding the role of gene expression in

adaptation to the most extreme environmental conditions on Earth for a warm-blooded vertebrate. In summary, through complementary analyses of a multi-tissue dataset, we were able to determine which tissues show the strongest signal of gene expression shifts in the Emperor penguin. We identified a prominent signature of the muscle and liver, and an apparent rewiring in the brain expression network. The lack of a gene expression signature in the skin suggests we should explore the role of coding sequence changes in this tissue. Future research on functions and roles of genes showing signals of divergence, either in expression or in coding sequence, is needed to better understand the initial phases of ecological divergence and rapid adaptation to novel selective constraints.

Acknowledgements

This study was supported by the Institut Polaire Français Paul-Emile Victor (IPEV) within the framework of the Program 137-ANTAVIA (PI: CLB), by the Centre Scientifique de Monaco with additional support from the LIA-647 and RTPI-NUTRESS (CSM/CNRS-UNISTRA), by the Centre National de la Recherche Scientifique (CNRS) through the Programme Zone Atelier de Recherches sur l'Environnement Antarctique et Subantarctique (ZATA). The study was approved by the French ethics committee (last: APAFIS#29338-2020070210516365) and the French Polar Environmental Committee, and permits to handle animals and access breeding sites were delivered by the "Terres Australes et Antarctiques Françaises" (TAAF). JRP is supported by funding from the European Union's Horizon Europe research and innovation programme under the Marie Skłodowska-Curie grant agreement No. 101068395 - 'Poly2Adapt'. SG was supported by PNRA16_00099 and PNRA16_00234. ET was supported by PNRA_16 00164 ("Programma Nazionale di Ricerca in Antartide". Bando PNRA 5 aprile 2016, n. 651. – Linea B "Genomica degli adattamenti estremi alla vita in Antartide"). Bioinformatic analyses were performed on the HPC clusters at the Department of Life and Environmental Sciences ("HappyComputing@DiSVA"), Marche Polytechnic University, and the Department of Life Sciences and Biotechnology, University of Ferrara.

References

Ancel, A., Kooyman, G. L., Ponganis, P. J., Gendner, J.-P., Lignon, J., Mestre, X., Huin, N., Thorson, P. H., Robisson, P., & Le Maho, Y. (1992). Foraging behaviour of emperor penguins as a resource detector in winter and summer. *Nature*, *360*(6402), 336–339. https://doi.org/10.1038/360336a0

Ancel, A., Visser, H., Handrich, Y., Masman, D., & Le Maho, Y. (1997). Energy saving in huddling penguins. *Nature*, *385*(6614), 304–305. https://doi.org/10.1038/385304a0

Andrews, S. (2010). *FastQC: A Quality Control Tool for High Throughput Sequence Data*. http://www.bioinformatics.babraham.ac.uk/projects/fastqc/

Bae, J. Y., Woo, J., Kang, S., & Shin, K. O. (2018). Effects of detraining and retraining on muscle energy-sensing network and meteorin-like levels in obese mice. *Lipids in Health and Disease*, *17*(1), 97. https://doi.org/10.1186/s12944-018-0751-3

Bell, E. M., & Callaghan, T. V. (2012). What are extreme environments and what lives in them? In *Life at extremes: environments, organisms and strategies for survival* (pp. 1–12). CABI. https://doi.org/10.1079/9781845938147.0001

Bénistant, C., Duchamp, C., Cohen-Adad, F., Rouanet, J. L., & Barré, H. (1998). Increased in vitro fatty acid supply and cellular transport capacities in cold-acclimated ducklings (Cairina moschata). *The American Journal of Physiology*, *275*(3), R683–R690. https://doi.org/10.1152/ajpregu.1998.275.3.R683

Bentz, A. B., Thomas, G. W. C., Rusch, D. B., & Rosvall, K. A. (2019). Tissue-specific expression profiles and positive selection analysis in the tree swallow (Tachycineta bicolor) using a de novo transcriptome assembly. *Scientific Reports*, *9*(1), 1–12. https://doi.org/10.1038/s41598-019-52312-4

Bickel, P. E., Tansey, J. T., & Welte, M. A. (2009). PAT proteins, an ancient family of lipid droplet proteins that regulate cellular lipid stores. *Biochimica et Biophysica Acta*, *1791*(6), 419–440. https://doi.org/10.1016/j.bbalip.2009.04.002

Bicudo, J. E., Vianna, C. R., & Chaui-Berlinck, J. G. (2001). Thermogenesis in birds. *Bioscience Reports*, *21*(2), 181–188. https://doi.org/10.1023/a:1013648208428

Bird, J. P., Martin, R., Akçakaya, H. R., Gilroy, J., Burfield, I. J., Garnett, S. T., Symes, A., Taylor, J., Şekercioğlu, Ç. H., & Butchart, S. H. M. (2020). Generation lengths of the world's birds and their implications for extinction risk. *Conservation Biology: The Journal of the Society for Conservation Biology*, *34*(5), 1252–1261. https://doi.org/10.1111/cobi.13486

Bley, N., Lederer, M., Pfalz, B., Reinke, C., Fuchs, T., Glaß, M., Möller, B., & Hüttelmaier, S. (2015). Stress granules are dispensable for mRNA stabilization during cellular stress. *Nucleic Acids Research*, *43*(4), e26. https://doi.org/10.1093/nar/gku1275

Blighe, K., Rana, S., & Lewis, M. (2018). *EnhancedVolcano: Publication-ready volcano plots with enhanced colouring and labeling*. https://github.com/kevinblighe/EnhancedVolcano

Botero, C. A., Weissing, F. J., Wright, J., & Rubenstein, D. R. (2015). Evolutionary tipping points in the capacity to adapt to environmental change. *Proceedings of the National Academy of Sciences of the United States of America*, *112*(1), 184–189. https://doi.org/10.1073/pnas.1408589111

Boyle, E. A., Li, Y. I., & Pritchard, J. K. (2017). An Expanded View of Complex Traits: From Polygenic to Omnigenic. *Cell*, *169*(7), 1177–1186. https://doi.org/10.1016/j.cell.2017.05.038

Brauer, C. J., Unmack, P. J., & Beheregaray, L. B. (2017). Comparative ecological transcriptomics and the contribution of gene expression to the evolutionary potential of a threatened fish. *Molecular Ecology*, *26*(24), 6841–6856. https://doi.org/10.1111/mec.14432

Braun, E. J. (2015). Chapter 12 - Osmoregulatory Systems of Birds. In C. G. Scanes (Ed.), *Sturkie's Avian Physiology (Sixth Edition)* (pp. 285–300). Academic Press. https://doi.org/10.1016/B978-0-12-407160-5.00012-9

Buchfink, B., Reuter, K., & Drost, H.-G. (2021). Sensitive protein alignments at tree-of-life scale using DIAMOND. *Nature Methods*, *18*(4), 366–368. https://doi.org/10.1038/s41592-021-01101-x

Burton, T., Ratikainen, I. I., & Einum, S. (2022). Environmental change and the rate of phenotypic plasticity. *Global Change Biology*, *28*(18), 5337–5345. https://doi.org/10.1111/gcb.16291

Bushmanova, E., Antipov, D., Lapidus, A., & Prjibelski, A. D. (2019). rnaSPAdes: a de novo transcriptome assembler and its application to RNA-Seq data. *GigaScience*, *8*(9), giz100. https://doi.org/10.1093/gigascience/giz100

Bushnell, B. (2014). *BBMap: A Fast, Accurate, Splice-Aware Aligner*. https://sourceforge.net/projects/bbmap/

Campbell-Staton, S. C., Cheviron, Z. A., Rochette, N., Catchen, J., Losos, J. B., & Edwards, S. V. (2017). Winter storms drive rapid phenotypic, regulatory, and genomic shifts in the green anole lizard. *Science*, *357*(6350), 495–498. https://doi.org/10.1126/science.aam5512

Cantalapiedra, C. P., Hernández-Plaza, A., Letunic, I., Bork, P., & Huerta-Cepas, J. (2021). eggNOG-mapper v2: Functional Annotation, Orthology Assignments, and Domain Prediction at the Metagenomic Scale. *Molecular Biology and Evolution*, *38*(12), 5825–5829. https://doi.org/10.1093/molbev/msab293

Chapin, F. S., Autumn, K., & Pugnaire, F. (1993). Evolution of Suites of Traits in Response to Environmental Stress. *The American Naturalist*, *142*, S78–S92. https://doi.org/10.1086/285524

Chen, J., Ren, X., Li, L., Lu, S., Chen, T., Tan, L., Liu, M., Luo, Q., Liang, S., Nie, Q., Zhang, X., & Luo, W. (2019). Integrative Analyses of mRNA Expression Profile Reveal the Involvement of IGF2BP1 in Chicken Adipogenesis. *International Journal of Molecular Sciences*, *20*(12).

https://doi.org/10.3390/ijms20122923

Chen, S., Zhou, Y., Chen, Y., & Gu, J. (2018). fastp: an ultra-fast all-in-one FASTQ preprocessor. *Bioinformatics* , *34*(17), i884–i890. https://doi.org/10.1093/bioinformatics/bty560

Cherel, Y., Robin, J.-P., & Maho, Y. L. (1988). Physiology and biochemistry of long-term fasting in birds. *Canadian Journal of Zoology*, *66*(1), 159–166. https://doi.org/10.1139/z88-022

Chesson, P., & Huntly, N. (1997). The roles of harsh and fluctuating conditions in the dynamics of ecological communities. *The American Naturalist*, *150*(5), 519–553. https://doi.org/10.1086/286080

Chevin, L.-M., & Hoffmann, A. A. (2017). Evolution of phenotypic plasticity in extreme environments. *Philosophical Transactions of the Royal Society of London. Series B, Biological Sciences*, *372*(1723). https://doi.org/10.1098/rstb.2016.0138

Chevin, L.-M., Lande, R., & Mace, G. M. (2010). Adaptation, plasticity, and extinction in a changing environment: towards a predictive theory. *PLoS Biology*, *8*(4), e1000357. https://doi.org/10.1371/journal.pbio.1000357

Choe, S. S., Huh, J. Y., Hwang, I. J., Kim, J. I., & Kim, J. B. (2016). Adipose Tissue Remodeling: Its Role in Energy Metabolism and Metabolic Disorders. *Frontiers in Endocrinology*, *7*, 30. https://doi.org/10.3389/fendo.2016.00030

Cho, H., Yang, Y. D., Lee, J., Lee, B., Kim, T., Jang, Y., Back, S. K., Na, H. S., Harfe, B. D., Wang, F., Raouf, R., Wood, J. N., & Oh, U. (2012). The calcium-activated chloride channel anoctamin 1 acts as a heat sensor in nociceptive neurons. *Nature Neuroscience*, *15*(7), 1015–1021. https://doi.org/10.1038/nn.3111

Cirera, S. (2013). Highly efficient method for isolation of total RNA from adipose tissue. *BMC Research Notes*, *6*, 472. https://doi.org/10.1186/1756-0500-6-472

Cole, T. L., Zhou, C., Fang, M., Pan, H., Ksepka, D. T., Fiddaman, S. R., Emerling, C. A., Thomas, D. B., Bi, X., Fang, Q., Ellegaard, M. R., Feng, S., Smith, A. L., Heath, T. A., Tennyson, A. J. D., Borboroglu, P. G., Wood, J. R., Hadden, P. W., Grosser, S., … Zhang, G. (2022). Genomic insights into the secondary aquatic transition of penguins. *Nature Communications*, *13*(1), 3912. https://doi.org/10.1038/s41467-022-31508-9

Corbel, H., Morlon, F., Geiger, S., & Groscolas, R. (2009). State-dependent decisions during the fledging process of king penguin chicks. *Animal Behaviour*, *78*(4), 829–838. https://doi.org/10.1016/j.anbehav.2009.06.019

Corley, S. M., Troy, N. M., Bosco, A., & Wilkins, M. R. (2019). QuantSeq. 3′ Sequencing

combined with Salmon provides a fast, reliable approach for high throughput RNA expression analysis. *Scientific Reports*, *9*(1), 1–15. https://doi.org/10.1038/s41598-019-55434-x

Corsolini, S., Nigro, M., Olmastroni, S., Focardi, S., & Regoli, F. (2001). Susceptibility to oxidative stress in Adélie and emperor penguin. *Polar Biology*, *24*(5), 365–368. https://doi.org/10.1007/s003000000220

Coulson-Thomas, V. J., Gesteira, T. F., Esko, J., & Kao, W. (2014). Heparan sulfate regulates hair follicle and sebaceous gland morphogenesis and homeostasis. *The Journal of Biological Chemistry*, *289*(36), 25211–25226. https://doi.org/10.1074/jbc.M114.572511

Davidson, E. H., & Erwin, D. H. (2006). Gene regulatory networks and the evolution of animal body plans. *Science*, *311*(5762), 796–800. https://doi.org/10.1126/science.1113832

Duchamp, C., & Barré, H. (1993). Skeletal muscle as the major site of nonshivering thermogenesis in cold-acclimated ducklings. *The American Journal of Physiology*, *265*(5 Pt 2), R1076–R1083. https://doi.org/10.1152/ajpregu.1993.265.5.R1076

Duchamp, C., Barré, H., Rouanet, J. L., Lanni, A., Cohen-Adad, F., Berne, G., & Brebion, P. (1991). Nonshivering thermogenesis in king penguin chicks. I. Role of skeletal muscle. *The American Journal of Physiology*, *261*(6 Pt 2), R1438–R1445. https://doi.org/10.1152/ajpregu.1991.261.6.R1438

Duchamp, C., Rouanet, J. L., & Barré, H. (2002). Ontogeny of thermoregulatory mechanisms in king penguin chicks (Aptenodytes patagonicus). *Comparative Biochemistry and Physiology. Part A, Molecular & Integrative Physiology*, *131*(4), 765–773. https://doi.org/10.1016/s1095-6433(02)00014-4

Fay, J. C., & Wittkopp, P. J. (2008). Evaluating the role of natural selection in the evolution of gene regulation. *Heredity*, *100*(2), 191–199. https://doi.org/10.1038/sj.hdy.6801000

Feld, S., & Hirschberg, R. (1996). Growth hormone, the insulin-like growth factor system, and the kidney. *Endocrine Reviews*, *17*(5), 423–480. https://doi.org/10.1210/edrv-17-5-423

Fenzl, A., Kulterer, O. C., Spirk, K., Mitulović, G., Marculescu, R., Bilban, M., Baumgartner-Parzer, S., Kautzky-Willer, A., Kenner, L., Plutzky, J., Quadro, L., & Kiefer, F. W. (2020). Intact vitamin A transport is critical for cold-mediated adipose tissue browning and thermogenesis. *Molecular Metabolism*, *42*, 101088. https://doi.org/10.1016/j.molmet.2020.101088

Finn, R. D., Bateman, A., Clements, J., Coggill, P., Eberhardt, R. Y., Eddy, S. R., Heger, A.,

Hetherington, K., Holm, L., Mistry, J., Sonnhammer, E. L. L., Tate, J., & Punta, M. (2014). Pfam: the protein families database. *Nucleic Acids Research*, *42*(Database issue), D222–D230. https://doi.org/10.1093/nar/gkt1223

Finn, R. D., Clements, J., & Eddy, S. R. (2011). HMMER web server: interactive sequence similarity searching. *Nucleic Acids Research*, *39*(Web Server issue), W29–W37. https://doi.org/10.1093/nar/gkr367

Fishman, B., & Tauber, E. (2023). Epigenetics and seasonal timing in animals: a concise review. *Journal of Comparative Physiology. A, Neuroethology, Sensory, Neural, and Behavioral Physiology*. https://doi.org/10.1007/s00359-023-01673-3

Fuentes, P., Pelletier, J., Martinez-Herráez, C., Diez-Obrero, V., Iannizzotto, F., Rubio, T., Garcia-Cajide, M., Menoyo, S., Moreno, V., Salazar, R., Tauler, A., & Gentilella, A. (2021). The 40*S*-LARP1 complex reprograms the cellular translatome upon mTOR inhibition to preserve the protein synthetic capacity. *Science Advances*, *7*(48), eabg9275. https://doi.org/10.1126/sciadv.abg9275

Gavryushkina, A., Heath, T. A., Ksepka, D. T., Stadler, T., Welch, D., & Drummond, A. J. (2017). Bayesian Total-Evidence Dating Reveals the Recent Crown Radiation of Penguins. *Systematic Biology*, *66*(1), 57–73. https://doi.org/10.1093/sysbio/syw060

Gilbert, C., Robertson, G., Le Maho, Y., Naito, Y., & Ancel, A. (2006). Huddling behavior in emperor penguins: Dynamics of huddling. *Physiology & Behavior*, *88*(4-5), 479–488. https://doi.org/10.1016/j.physbeh.2006.04.024

Giménez-Cassina, A., & Danial, N. N. (2015). Regulation of mitochondrial nutrient and energy metabolism by BCL-2 family proteins. *Trends in Endocrinology and Metabolism: TEM*, *26*(4), 165–175. https://doi.org/10.1016/j.tem.2015.02.004

Grabherr, M. G., Haas, B. J., Yassour, M., Levin, J. Z., Thompson, D. A., Amit, I., Adiconis, X., Fan, L., Raychowdhury, R., Zeng, Q., Chen, Z., Mauceli, E., Hacohen, N., Gnirke, A., Rhind, N., di Palma, F., Birren, B. W., Nusbaum, C., Lindblad-Toh, K., … Regev, A. (2011). Full-length transcriptome assembly from RNA-Seq data without a reference genome. *Nature Biotechnology*, *29*(7), 644–652. https://doi.org/10.1038/nbt.1883

Graja, A., Garcia-Carrizo, F., Jank, A.-M., Gohlke, S., Ambrosi, T. H., Jonas, W., Ussar, S., Kern, M., Schürmann, A., Aleksandrova, K., Blüher, M., & Schulz, T. J. (2018). Loss of periostin occurs in aging adipose tissue of mice and its genetic ablation impairs adipose tissue lipid metabolism. *Aging Cell*, *17*(5), e12810. https://doi.org/10.1111/acel.12810

Grant, P. R., Grant, B. R., Huey, R. B., Johnson, M. T. J., Knoll, A. H., & Schmitt, J. (2017). Evolution caused by extreme events. *Philosophical Transactions of the Royal Society of London. Series B, Biological Sciences*, *372*(1723). https://doi.org/10.1098/rstb.2016.0146

Grifone, R., Demignon, J., Giordani, J., Niro, C., Souil, E., Bertin, F., Laclef, C., Xu, P.-X., & Maire, P. (2007). Eya1 and Eya2 proteins are required for hypaxial somitic myogenesis in the mouse embryo. *Developmental Biology*, *302*(2), 602–616. https://doi.org/10.1016/j.ydbio.2006.08.059

Grifone, R., Laclef, C., Spitz, F., Lopez, S., Demignon, J., Guidotti, J.-E., Kawakami, K., Xu, P.-X., Kelly, R., Petrof, B. J., Daegelen, D., Concordet, J.-P., & Maire, P. (2004). Six1 and Eya1 expression can reprogram adult muscle from the slow-twitch phenotype into the fast-twitch phenotype. *Molecular and Cellular Biology*, *24*(14), 6253–6267. https://doi.org/10.1128/MCB.24.14.6253-6267.2004

Groscolas, R. (1990). Metabolic adaptations to fasting in emperor and king penguins. *Penguin Biology*.

Groscolas, R., & Leloup, J. (1986). The endocrine control of reproduction and molt in male and female emperor (Aptenodytes forsteri) and adelie (Pygoscelis adeliae) penguins. II. Annual changes in plasma levels of thyroxine and triiodothyronine. *General and Comparative Endocrinology*, *63*(2), 264–274. https://doi.org/10.1016/0016-6480(86)90164-4

Groscolas, R., & Robin, J. P. (2001). Long-term fasting and re-feeding in penguins. *Comparative Biochemistry and Physiology. Part A, Molecular & Integrative Physiology*, *128*(3), 645–655. https://doi.org/10.1016/s1095-6433(00)00341-x

GTEx Consortium. (2015). Human genomics. The Genotype-Tissue Expression (GTEx) pilot analysis: multitissue gene regulation in humans. *Science*, *348*(6235), 648–660. https://doi.org/10.1126/science.1262110

Haas, B. J., Papanicolaou, A., Yassour, M., Grabherr, M., Blood, P. D., Bowden, J., Couger, M. B., Eccles, D., Li, B., Lieber, M., MacManes, M. D., Ott, M., Orvis, J., Pochet, N., Strozzi, F., Weeks, N., Westerman, R., William, T., Dewey, C. N., … Regev, A. (2013). De novo transcript sequence reconstruction from RNA-seq using the Trinity platform for reference generation and analysis. *Nature Protocols*, *8*(8), 1494–1512. https://doi.org/10.1038/nprot.2013.084

Heller, E., & Fuchs, E. (2015). Tissue patterning and cellular mechanics. *The Journal of Cell*

Biology, *211*(2), 219–231. https://doi.org/10.1083/jcb.201506106

Hirschberg, R., & Kopple, J. D. (1989). Evidence that insulin-like growth factor I increases renal plasma flow and glomerular filtration rate in fasted rats. *The Journal of Clinical Investigation*, *83*(1), 326–330. https://doi.org/10.1172/JCI113878

Hoffmann, A. A., & Hercus, M. J. (2000). Environmental Stress as an Evolutionary Force. *Bioscience*, *50*(3), 217–226. https://doi.org/10.1641/0006-3568(2000)050[0217:ESAAEF]2.3.CO;2

Hoffmann, A. A., & Parsons, P. A. (1997). *Extreme Environmental Change and Evolution*. Cambridge University Press. https://play.google.com/store/books/details?id=XqjTTDPkb5sC

Hoffmann, A. A., Sørensen, J. G., & Loeschcke, V. (2003). Adaptation of Drosophila to temperature extremes: bringing together quantitative and molecular approaches. *Journal of Thermal Biology*, *28*(3), 175–216. https://doi.org/10.1016/S0306-4565(02)00057-8

Hohtola, E. (2002). Facultative and obligatory thermogenesis in young birds: a cautionary note. *Comparative Biochemistry and Physiology. Part A, Molecular & Integrative Physiology*, *131*(4), 733–739. https://doi.org/10.1016/s1095-6433(02)00011-9

Jackson, S. T., Betancourt, J. L., Booth, R. K., & Gray, S. T. (2009). Ecology and the ratchet of events: climate variability, niche dimensions, and species distributions. *Proceedings of the National Academy of Sciences of the United States of America*, *106 Suppl 2*(Suppl 2), 19685–19692. https://doi.org/10.1073/pnas.0901644106

Jhiang, S. M. (2000). The RET proto-oncogene in human cancers. *Oncogene*. https://idp.nature.com/authorize/casa?redirect_uri=https://www.nature.com/articles/1203857&casa_token=Jwmef10O8UEAAAAA:E0qYvzvb1dLvpsymNjOXgWEMzJuUkvX_uVVQMoUcVCMX1sxi3LH9OdPuYT_txZu17zI0NE9vy58yN7K5zu0

Jones, F. C., Grabherr, M. G., Chan, Y. F., Russell, P., Mauceli, E., Johnson, J., Swofford, R., Pirun, M., Zody, M. C., White, S., Birney, E., Searle, S., Schmutz, J., Grimwood, J., Dickson, M. C., Myers, R. M., Miller, C. T., Summers, B. R., Knecht, A. K., … Kingsley, D. M. (2012). The genomic basis of adaptive evolution in threespine sticklebacks. *Nature*, *484*(7392), 55–61. https://doi.org/10.1038/nature10944

Josephs, E. B. (2021). Gene expression links genotype and phenotype during rapid adaptation [Review of *Gene expression links genotype and phenotype during rapid adaptation*]. *Molecular Ecology*, *30*(1), 30–32. Wiley Online Library. https://doi.org/10.1111/mec.15729

Kannan, S., Hui, J., Mazooji, K., Pachter, L., & Tse, D. (2016). Shannon: An Information-Optimal de Novo RNA-Seq Assembler. In *bioRxiv* (p. 039230). https://doi.org/10.1101/039230

Kim, D.-H., Sarbassov, D. D., Ali, S. M., King, J. E., Latek, R. R., Erdjument-Bromage, H., Tempst, P., & Sabatini, D. M. (2002). mTOR interacts with raptor to form a nutrient-sensitive complex that signals to the cell growth machinery. *Cell*, *110*(2), 163–175. https://doi.org/10.1016/s0092-8674(02)00808-5

Klingenspor, M. (2003). Cold-induced recruitment of brown adipose tissue thermogenesis. *Experimental Physiology*, *88*(1), 141–148. https://doi.org/10.1113/eph8802508

Kooyman, G. L. (1993). Breeding habitats of emperor penguins in the western Ross Sea. *Antarctic Science / Blackwell Scientific Publications*, *5*(2), 143–148. https://doi.org/10.1017/S0954102093000203

Kozaki, Y., Umetsu, R., Mizukami, Y., Yamamura, A., Kitamori, K., Tsuchikura, S., Ikeda, K., & Yamori, Y. (2015). Peripheral gene expression profile of mechanical hyperalgesia induced by repeated cold stress in SHRSP5/Dmcr rats. *The Journal of Physiological Sciences: JPS*, *65*(5), 417–425. https://doi.org/10.1007/s12576-015-0380-9

Kriventseva, E. V., Kuznetsov, D., Tegenfeldt, F., Manni, M., Dias, R., Simão, F. A., & Zdobnov, E. M. (2019). OrthoDB v10: sampling the diversity of animal, plant, fungal, protist, bacterial and viral genomes for evolutionary and functional annotations of orthologs. *Nucleic Acids Research*, *47*(D1), D807–D811. https://doi.org/10.1093/nar/gky1053

Krogh, A., Larsson, B., von Heijne, G., & Sonnhammer, E. L. (2001). Predicting transmembrane protein topology with a hidden Markov model: application to complete genomes. *Journal of Molecular Biology*, *305*(3), 567–580. https://doi.org/10.1006/jmbi.2000.4315

Langfelder, P., & Horvath, S. (2008). WGCNA: an R package for weighted correlation network analysis. *BMC Bioinformatics*, *9*, 559. https://doi.org/10.1186/1471-2105-9-559

Langfelder, P., & Horvath, S. (2012). Fast R Functions for Robust Correlations and Hierarchical Clustering. *Journal of Statistical Software*, *46*(11). https://doi.org/10.18637/jss.v046.i11

Langfelder, P., Luo, R., Oldham, M. C., & Horvath, S. (2011). Is my network module preserved and reproducible? *PLoS Computational Biology*, *7*(1), e1001057. https://doi.org/10.1371/journal.pcbi.1001057

Lee, J. O., Byun, W. S., Kang, M. J., Han, J. A., Moon, J., Shin, M.-J., Lee, H. J., Chung, J. H., Lee, J.-S., Son, C.-G., Song, K.-H., Kim, T. W., Lee, E.-S., Kim, H. M., Chung, C. H., Ngoei, K. R. W., Ling, N. X. Y., Oakhill, J. S., Galic, S., … Kim, H. S. (2020). The myokine meteorin-like

(metrnl) improves glucose tolerance in both skeletal muscle cells and mice by targeting AMPKα2. *The FEBS Journal*, *287*(10), 2087–2104. https://doi.org/10.1111/febs.15301

Lekevičius, E. (2009). Vacant niches in nature, ecology, and evolutionary theory: a mini-review. In *Ekologija*. elekevicius.lt. https://doi.org/10.2478/v10055-009-0020-x

Le Maho, Y. (1977a). The Emperor Penguin: A Strategy to Live and Breed in the Cold: Morphology, physiology, ecology, and behavior distinguish the polar emperor penguin from other penguin species, particularly from its close relative, the king penguin. *American Scientist*, *65*(6), 680–693. http://www.jstor.org/stable/27848168

Le Maho, Y. (1977b). The Emperor Penguin: A Strategy to Live and Breed in the Cold: Morphology, physiology, ecology, and behavior distinguish the polar emperor penguin from other penguin species, particularly from its close relative, the king penguin. *American Scientist*, *65*(6), 680–693. http://www.jstor.org/stable/27848168

Le Maho, Y., Delclitte, P., & Chatonnet, J. (1976). Thermoregulation in fasting emperor penguins under natural conditions. *The American Journal of Physiology*, *231*(3), 913–922. https://doi.org/10.1152/ajplegacy.1976.231.3.913

Levis, N. A., & Pfennig, D. W. (2016). Evaluating “Plasticity-First” Evolution in Nature: Key Criteria and Empirical Approaches. *Trends in Ecology & Evolution*, *31*(7), 563–574. https://doi.org/10.1016/j.tree.2016.03.012

Lewden, A., Enstipp, M. R., Picard, B., van Walsum, T., & Handrich, Y. (2017). High peripheral temperatures in king penguins while resting at sea: thermoregulation versus fat deposition. *The Journal of Experimental Biology*, *220*(Pt 17), 3084–3094. https://doi.org/10.1242/jeb.158980

Li, C., Zhang, Y., Li, J., Kong, L., Hu, H., Pan, H., Xu, L., Deng, Y., Li, Q., Jin, L., Yu, H., Chen, Y., Liu, B., Yang, L., Liu, S., Zhang, Y., Lang, Y., Xia, J., He, W., ... Zhang, G. (2014). Two Antarctic penguin genomes reveal insights into their evolutionary history and molecular changes related to the Antarctic environment. *GigaScience*, *3*(1), 27. https://doi.org/10.1186/2047-217X-3-27

Li, J., Dong, Y., Lü, X., Wang, L., Peng, W., Zhang, X. C., & Rao, Z. (2013). Crystal structures and biochemical studies of human lysophosphatidic acid phosphatase type 6. *Protein & Cell*, *4*(7), 548–561. https://doi.org/10.1007/s13238-013-3031-z

Lisse, T. S., & Hewison, M. (2011). Vitamin D: a new player in the world of mTOR signaling. *Cell Cycle* , *10*(12), 1888–1889. https://doi.org/10.4161/cc.10.12.15620

Liu, S., Lorenzen, E. D., Fumagalli, M., Li, B., Harris, K., Xiong, Z., Zhou, L., Korneliussen, T. S., Somel, M., Babbitt, C., Wray, G., Li, J., He, W., Wang, Z., Fu, W., Xiang, X., Morgan, C. C., Doherty, A., O'Connell, M. J., … Wang, J. (2014). Population genomics reveal recent speciation and rapid evolutionary adaptation in polar bears. *Cell*, *157*(4), 785–794. https://doi.org/10.1016/j.cell.2014.03.054

Lopez, J., & Tait, S. W. G. (2015). Mitochondrial apoptosis: killing cancer using the enemy within. *British Journal of Cancer*, *112*(6), 957–962. https://doi.org/10.1038/bjc.2015.85

Love, M. I., Huber, W., & Anders, S. (2014). Moderated estimation of fold change and dispersion for RNA-seq data with DESeq2. *Genome Biology*, *15*(12), 550. https://doi.org/10.1186/s13059-014-0550-8

MacManes, M. D. (2018). The Oyster River Protocol: a multi-assembler and kmer approach for de novo transcriptome assembly. *PeerJ*, *6*, e5428. https://doi.org/10.7717/peerj.5428

Mattick, J. S., Amaral, P. P., Carninci, P., Carpenter, S., Chang, H. Y., Chen, L.-L., Chen, R., Dean, C., Dinger, M. E., Fitzgerald, K. A., Gingeras, T. R., Guttman, M., Hirose, T., Huarte, M., Johnson, R., Kanduri, C., Kapranov, P., Lawrence, J. B., Lee, J. T., … Wu, M. (2023). Long non-coding RNAs: definitions, functions, challenges and recommendations. *Nature Reviews. Molecular Cell Biology*, 1–17. https://doi.org/10.1038/s41580-022-00566-8

Metzger, D. C. H., & Schulte, P. M. (2018). Similarities in temperature-dependent gene expression plasticity across timescales in threespine stickleback (Gasterosteus aculeatus). *Molecular Ecology*, *27*(10), 2381–2396. https://doi.org/10.1111/mec.14591

Mezentseva, N. V., Kumaratilake, J. S., & Newman, S. A. (2008). The brown adipocyte differentiation pathway in birds: an evolutionary road not taken. *BMC Biology*, *6*, 17. https://doi.org/10.1186/1741-7007-6-17

Miché, F., Vivien-Roels, B., Pévet, P., Spehner, C., Robin, J. P., & Le Maho, Y. (1991). Daily pattern of melatonin secretion in an antarctic bird, the emperor penguin, Aptenodytes forsteri: seasonal variations, effect of constant illumination and of administration of isoproterenol or propranolol. *General and Comparative Endocrinology*, *84*(2), 249–263. https://doi.org/10.1016/0016-6480(91)90048-b

Mitra, V., & Metcalf, J. (2012). Metabolic functions of the liver. *Anaesthesia & Intensive Care Medicine*, *13*(2), 54–55. https://doi.org/10.1016/j.mpaic.2011.11.006

Mo, D., Yu, K., Chen, H., Chen, L., Liu, X., He, Z., Cong, P., & Chen, Y. (2017). Transcriptome Landscape of Porcine Intramuscular Adipocytes during Differentiation. *Journal of*

Agricultural and Food Chemistry, *65*(30), 6317–6328. https://doi.org/10.1021/acs.jafc.7b02039

Moll, P., Ante, M., Seitz, A., & Reda, T. (2014). QuantSeq 3′ mRNA sequencing for RNA quantification. *Nature Methods*, *11*(12), i – iii. https://doi.org/10.1038/nmeth.f.376

Nakamura, K., & Morrison, S. F. (2011). Central efferent pathways for cold-defensive and febrile shivering. *The Journal of Physiology*, *589*(Pt 14), 3641–3658. https://doi.org/10.1113/jphysiol.2011.210047

Nawrocki, E. P., & Eddy, S. R. (2013). Infernal 1.1: 100-fold faster RNA homology searches. *Bioinformatics* , *29*(22), 2933–2935. https://doi.org/10.1093/bioinformatics/btt509

Newman, S. A. (2011). Thermogenesis, muscle hyperplasia, and the origin of birds. *BioEssays: News and Reviews in Molecular, Cellular and Developmental Biology*, *33*(9), 653–656. https://doi.org/10.1002/bies.201100061

Oldham, M. C., Horvath, S., & Geschwind, D. H. (2006). Conservation and evolution of gene coexpression networks in human and chimpanzee brains. *Proceedings of the National Academy of Sciences of the United States of America*, *103*(47), 17973–17978. https://doi.org/10.1073/pnas.0605938103

Paris, J., Nitta Fernandes, F. A., Pirri, F., Greco, S., Gerdol, M., Pallavicini, A., Benoiste, M., Cornec, C., Zane, L., Haas, B., Le Bohec, C., & Trucchi, E. (2023). *josieparis/EP-KP-transcriptomics: v1.0* (Version v1.0). Zenodo. https://doi.org/10.5281/zenodo.10218729

Patro, R., Duggal, G., Love, M. I., Irizarry, R. A., & Kingsford, C. (2017). Salmon provides fast and bias-aware quantification of transcript expression. *Nature Methods*, *14*(4), 417–419. https://doi.org/10.1038/nmeth.4197

Pavey, S. A., Collin, H., Nosil, P., & Rogers, S. M. (2010). The role of gene expression in ecological speciation. *Annals of the New York Academy of Sciences*, *1206*(1), 110–129. https://doi.org/10.1111/j.1749-6632.2010.05765.x

Periasamy, M., Herrera, J. L., & Reis, F. C. G. (2017). Skeletal Muscle Thermogenesis and Its Role in Whole Body Energy Metabolism. *Diabetes & Metabolism Journal*, *41*(5), 327–336. https://doi.org/10.4093/dmj.2017.41.5.327

Petrenko, A. B., Yamakura, T., Baba, H., & Shimoji, K. (2003). The Role of N-Methyl-d-Aspartate (NMDA) Receptors in Pain: A Review. *Anesthesia & Analgesia*, *97*(4), 1108. https://doi.org/10.1213/01.ANE.0000081061.12235.55

Petropoulos, H., Gianakopoulos, P. J., Ridgeway, A. G., & Skerjanc, I. S. (2004). Disruption of

Meox or Gli activity ablates skeletal myogenesis in P19 cells. *The Journal of Biological Chemistry*, *279*(23), 23874–23881. https://doi.org/10.1074/jbc.M312612200

Pfenninger, M., Foucault, Q., Waldvogel, A.-M., & Feldmeyer, B. (2023). Selective effects of a short transient environmental fluctuation on a natural population. *Molecular Ecology*, *32*(2), 335–349. https://doi.org/10.1111/mec.16748

Pirri, F., Ometto, L., Fuselli, S., Fernandes, F. A. N., Ancona, L., Perta, N., Di Marino, D., Le Bohec, C., Zane, L., & Trucchi, E. (2022). Selection-driven adaptation to the extreme Antarctic environment in the Emperor penguin. *Heredity*. https://doi.org/10.1038/s41437-022-00564-8

Ponganis, P. J., Van Dam, R. P., Levenson, D. H., Knower, T., Ponganis, K. V., & Marshall, G. (2003). Regional heterothermy and conservation of core temperature in emperor penguins diving under sea ice. *Comparative Biochemistry and Physiology. Part A, Molecular & Integrative Physiology*, *135*(3), 477–487. https://doi.org/10.1016/s1095-6433(03)00133-8

Prévost, J. (1961). *L'écologie du Manchot empereur Aptenodytes forsteri (Gray)*. Éditions Scientifiques Hermann. https://books.google.it/books?id=rfYiygAACAAJ

Qi, X., Zhang, Q., He, Y., Yang, L., Zhang, X., Shi, P., Yang, L., Liu, Z., Zhang, F., Liu, F., Liu, S., Wu, T., Cui, C., Ouzhuluobu, Bai, C., Baimakangzhuo, Han, J., Zhao, S., Liang, C., & Su, B. (2019). The Transcriptomic Landscape of Yaks Reveals Molecular Pathways for High Altitude Adaptation. *Genome Biology and Evolution*, *11*(1), 72–85. https://doi.org/10.1093/gbe/evy264

Radomski, M. W., & Orme, T. (1971). Response of lipoprotein lipase in various tissues to cold exposure. *The American Journal of Physiology*, *220*(6), 1852–1856. https://doi.org/10.1152/ajplegacy.1971.220.6.1852

Raimbault, S., Dridi, S., Denjean, F., Lachuer, J., Couplan, E., Bouillaud, F., Bordas, A., Duchamp, C., Taouis, M., & Ricquier, D. (2001). An uncoupling protein homologue putatively involved in facultative muscle thermogenesis in birds. *Biochemical Journal*, *353*(Pt 3), 441–444. https://doi.org/10.1042/0264-6021:3530441

Rao, R. R., Long, J. Z., White, J. P., Svensson, K. J., Lou, J., Lokurkar, I., Jedrychowski, M. P., Ruas, J. L., Wrann, C. D., Lo, J. C., Camera, D. M., Lachey, J., Gygi, S., Seehra, J., Hawley, J. A., & Spiegelman, B. M. (2014). Meteorin-like is a hormone that regulates immune-adipose interactions to increase beige fat thermogenesis. *Cell*, *157*(6), 1279–1291.

https://doi.org/10.1016/j.cell.2014.03.065

Rappaport, N., Nativ, N., Stelzer, G., Twik, M., Guan-Golan, Y., Stein, T. I., Bahir, I., Belinky, F., Morrey, C. P., Safran, M., & Lancet, D. (2013). MalaCards: an integrated compendium for diseases and their annotation. *Database: The Journal of Biological Databases and Curation*, *2013*, bat018. https://doi.org/10.1093/database/bat018

Ribot, J., Felipe, F., Bonet, M. L., & Palou, A. (2004). Retinoic acid administration and vitamin A status modulate retinoid X receptor alpha and retinoic acid receptor alpha levels in mouse brown adipose tissue. *Molecular and Cellular Biochemistry*, *266*(1-2), 25–30. https://doi.org/10.1023/b:mcbi.0000049129.29612.14

Robin, J.-P., Boucontet, L., Chillet, P., & Groscolas, R. (1998). Behavioral changes in fasting emperor penguins: evidence for a “refeeding signal” linked to a metabolic shift. *American Journal of Physiology-Regulatory, Integrative and Comparative Physiology*, *274*(3), R746–R753. https://doi.org/10.1152/ajpregu.1998.274.3.R746

Robin, J.-P., Frain, M., Sardet, C., Groscolas, R., & Le Maho, Y. (1988). Protein and lipid utilization during long-term fasting in emperor penguins. *American Journal of Physiology-Regulatory, Integrative and Comparative Physiology*, *254*(1), R61–R68. https://doi.org/10.1152/ajpregu.1988.254.1.R61

Rothschild, L. J., & Mancinelli, R. L. (2001). Life in extreme environments. *Nature*, *409*(6823), 1092–1101. https://doi.org/10.1038/35059215

Rowland, L. A., Bal, N. C., & Periasamy, M. (2015). The role of skeletal-muscle-based thermogenic mechanisms in vertebrate endothermy. *Biological Reviews of the Cambridge Philosophical Society*, *90*(4), 1279–1297. https://doi.org/10.1111/brv.12157

Sarapio, E., De Souza, S. K., Model, J. F. A., Trapp, M., & Da Silva, R. S. M. (2019). Stanniocalcin-1 and -2 effects on glucose and lipid metabolism in white adipose tissue from fed and fasted rats. *Canadian Journal of Physiology and Pharmacology*, *97*(10), 916–923. https://doi.org/10.1139/cjpp-2019-0023

Scheiner, S. M. (1993). Genetics and Evolution of Phenotypic Plasticity. *Annual Review of Ecology and Systematics*, *24*(1), 35–68. https://doi.org/10.1146/annurev.es.24.110193.000343

Scheiner, S. M., & Lyman, R. F. (1989). The genetics of phenotypic plasticity I. Heritability. *Journal of Evolutionary Biology*, *2*(2), 95–107. https://doi.org/10.1046/j.1420-9101.1989.2020095.x

Sebag, S. C., Zhang, Z., Qian, Q., Li, M., Zhu, Z., Harata, M., Li, W., Zingman, L. V., Liu, L., Lira, V. A., Potthoff, M. J., Bartelt, A., & Yang, L. (2021). ADH5-mediated NO bioactivity maintains metabolic homeostasis in brown adipose tissue. *Cell Reports*, *37*(7), 110003. https://doi.org/10.1016/j.celrep.2021.110003

Shamsi, F., Wang, C.-H., & Tseng, Y.-H. (2021). The evolving view of thermogenic adipocytes - ontogeny, niche and function. *Nature Reviews. Endocrinology*, *17*(12), 726–744. https://doi.org/10.1038/s41574-021-00562-6

Simão, F. A., Waterhouse, R. M., Ioannidis, P., Kriventseva, E. V., & Zdobnov, E. M. (2015). BUSCO: assessing genome assembly and annotation completeness with single-copy orthologs. *Bioinformatics* , *31*(19), 3210–3212. https://doi.org/10.1093/bioinformatics/btv351

Simpson, G. G. (1946). *Fossil penguins*. *87*, 7–99.

Simpson, G. G. (1976). *Penguins : past and present, here and there*. cir.nii.ac.jp. https://cir.nii.ac.jp/crid/1130000079174472448

Sinitsky, M. Y., Matveeva, V. G., Asanov, M. A., & Ponasenko, A. V. (2018). Modifications in routine protocol of RNA isolation can improve quality of RNA purified from adipocytes. *Analytical Biochemistry*, *543*, 128–131. https://doi.org/10.1016/j.ab.2017.12.020

Sjöstedt, E., Zhong, W., Fagerberg, L., Karlsson, M., Mitsios, N., Adori, C., Oksvold, P., Edfors, F., Limiszewska, A., Hikmet, F., Huang, J., Du, Y., Lin, L., Dong, Z., Yang, L., Liu, X., Jiang, H., Xu, X., Wang, J., … Mulder, J. (2020). An atlas of the protein-coding genes in the human, pig, and mouse brain. *Science*, *367*(6482). https://doi.org/10.1126/science.aay5947

Smith, L. R., Meyer, G., & Lieber, R. L. (2013). Systems analysis of biological networks in skeletal muscle function. *Wiley Interdisciplinary Reviews. Systems Biology and Medicine*, *5*(1), 55–71. https://doi.org/10.1002/wsbm.1197

Smith-Unna, R., Boursnell, C., Patro, R., Hibberd, J. M., & Kelly, S. (2016). TransRate: reference-free quality assessment of de novo transcriptome assemblies. *Genome Research*, *26*(8), 1134–1144. https://doi.org/10.1101/gr.196469.115

Söhle, J., Machuy, N., Smailbegovic, E., Holtzmann, U., Grönniger, E., Wenck, H., Stäb, F., & Winnefeld, M. (2012). Identification of new genes involved in human adipogenesis and fat storage. *PloS One*, *7*(2), e31193. https://doi.org/10.1371/journal.pone.0031193

Song, L., & Florea, L. (2015). Rcorrector: efficient and accurate error correction for Illumina RNA-seq reads. *GigaScience*, *4*, 48. https://doi.org/10.1186/s13742-015-0089-y

Sparr, R., Braun, E. J., & Sweazea, K. L. (2010). Putative role for insulin in glucose regulation by avian kidneys. *FASEB Journal: Official Publication of the Federation of American Societies for Experimental Biology*, *24*(S1). https://doi.org/10.1096/fasebj.24.1_supplement.lb614

Steinhoff, J. S., Lass, A., & Schupp, M. (2022). Retinoid Homeostasis and Beyond: How Retinol Binding Protein 4 Contributes to Health and Disease. *Nutrients*, *14*(6), 1236. https://doi.org/10.3390/nu14061236

Stomberski, C. T., Hess, D. T., & Stamler, J. S. (2019). Protein S-Nitrosylation: Determinants of Specificity and Enzymatic Regulation of S-Nitrosothiol-Based Signaling. *Antioxidants & Redox Signaling*, *30*(10), 1331–1351. https://doi.org/10.1089/ars.2017.7403

Stonehouse, B. (1969). Environmental temperatures of tertiary penguins. *Science*, *163*(3868), 673–675. https://doi.org/10.1126/science.163.3868.673

Sun, Y., Zhao, G., Liu, R., Zheng, M., Hu, Y., Wu, D., Zhang, L., Li, P., & Wen, J. (2013). The identification of 14 new genes for meat quality traits in chicken using a genome-wide association study. *BMC Genomics*, *14*, 458. https://doi.org/10.1186/1471-2164-14-458

Swanson, D. L., Zhang, Y., & Jimenez, A. G. (2022). Skeletal muscle and metabolic flexibility in response to changing energy demands in wild birds. *Frontiers in Physiology*, *13*, 961392. https://doi.org/10.3389/fphys.2022.961392

Talbot, D. A., Duchamp, C., Rey, B., Hanuise, N., Rouanet, J. L., Sibille, B., & Brand, M. D. (2004). Uncoupling protein and ATP/ADP carrier increase mitochondrial proton conductance after cold adaptation of king penguins. *The Journal of Physiology*, *558*(Pt 1), 123–135. https://doi.org/10.1113/jphysiol.2004.063768

Taylor, J. R. E. (1986). Thermal Insulation of the Down and Feathers of Pygoscelid Penguin Chicks and the Unique Properties of Penguin Feathers. *The Auk*, *103*(1), 160–168. https://doi.org/10.1093/auk/103.1.160

Teufel, F., Almagro Armenteros, J. J., Johansen, A. R., Gíslason, M. H., Pihl, S. I., Tsirigos, K. D., Winther, O., Brunak, S., von Heijne, G., & Nielsen, H. (2022). SignalP 6.0 predicts all five types of signal peptides using protein language models. *Nature Biotechnology*, *40*(7), 1023–1025. https://doi.org/10.1038/s41587-021-01156-3

Teulier, L., Rouanet, J.-L., Letexier, D., Romestaing, C., Belouze, M., Rey, B., Duchamp, C., & Roussel, D. (2010). Cold-acclimation-induced non-shivering thermogenesis in birds is associated with upregulation of avian UCP but not with innate uncoupling or altered ATP

efficiency. *The Journal of Experimental Biology*, *213*(Pt 14), 2476–2482. https://doi.org/10.1242/jeb.043489

Teulier, L., Rouanet, J.-L., Rey, B., & Roussel, D. (2014). Ontogeny of non-shivering thermogenesis in Muscovy ducklings (Cairina moschata). *Comparative Biochemistry and Physiology. Part A, Molecular & Integrative Physiology*, *175*, 82–89. https://doi.org/10.1016/j.cbpa.2014.05.012

Thomas, D. B., Ksepka, D. T., & Fordyce, R. E. (2011). Penguin heat-retention structures evolved in a greenhouse Earth. *Biology Letters*, *7*(3), 461–464. https://doi.org/10.1098/rsbl.2010.0993

Tinker, D. A., Brosnan, J. T., & Herzberg, G. R. (1984). Metabolite levels in fed and fasted chicken liver and kidney while employing a technique for artificial respiration in birds. *Comparative Biochemistry and Physiology Part B: Comparative Biochemistry*, *77*(1), 119–124. https://doi.org/10.1016/0305-0491(84)90232-3

Tobler, M., Kelley, J. L., Plath, M., & Riesch, R. (2018). Extreme environments and the origins of biodiversity: Adaptation and speciation in sulphide spring fishes. *Molecular Ecology*, *27*(4), 843–859. https://doi.org/10.1111/mec.14497

Tripodi, A., Lombardi, R., Primignani, M., La Mura, V., Peyvandi, F., & Fracanzani, A. L. (2022). Hypercoagulability in Patients with Non-Alcoholic Fatty Liver Disease (NAFLD): Causes and Consequences. *Biomedicines*, *10*(2). https://doi.org/10.3390/biomedicines10020249

Uusi-Heikkilä, S., Sävilammi, T., Leder, E., Arlinghaus, R., & Primmer, C. R. (2017). Rapid, broad-scale gene expression evolution in experimentally harvested fish populations. *Molecular Ecology*, *26*(15), 3954–3967. https://doi.org/10.1111/mec.14179

Valenti, L., Tripodi, A., La Mura, V., Pelusi, S., Bianco, C., Scalambrino, E., Margarita, S., Malvestiti, F., Ronzoni, L., Clerici, M., D'Ambrosio, R., Fraquelli, M., Carpani, R., Prati, D., & Peyvandi, F. (2022). Clinical and genetic determinants of the fatty liver-coagulation balance interplay in individuals with metabolic dysfunction. *JHEP Reports : Innovation in Hepatology*, *4*(12), 100598. https://doi.org/10.1016/j.jhepr.2022.100598

Vianna, J. A., Fernandes, F. A. N., Frugone, M. J., Figueiró, H. V., Pertierra, L. R., Noll, D., Bi, K., Wang-Claypool, C. Y., Lowther, A., Parker, P., Le Bohec, C., Bonadonna, F., Wienecke, B., Pistorius, P., Steinfurth, A., Burridge, C. P., Dantas, G. P. M., Poulin, E., Simison, W. B., … Bowie, R. C. K. (2020). Genome-wide analyses reveal drivers of penguin diversification. *Proceedings of the National Academy of Sciences of the United States of America*,

117(36), 22303–22310. https://doi.org/10.1073/pnas.2006659117

Via, S., & Lande, R. (1985). Genotype-environment interaction and the evolution of phenotypic plasticity. *Evolution; International Journal of Organic Evolution*, *39*(3), 505–522. https://doi.org/10.1111/j.1558-5646.1985.tb00391.x

Vriens, J., Nilius, B., & Voets, T. (2014). Peripheral thermosensation in mammals. *Nature Reviews. Neuroscience*, *15*(9), 573–589. https://doi.org/10.1038/nrn3784

Wakatsuki, K., T-Uchimura, Y., Matsubara, T., Nasu, T., Mizumura, K., & Taguchi, T. (2021). Peripheral nociceptive mechanisms in an experimental rat model of fibromyalgia induced by repeated cold stress. *Neuroscience Research*, *162*, 22–30. https://doi.org/10.1016/j.neures.2019.12.015

Wang, Z., Kontani, Y., Sato, Y., Mizuno, T., Mori, N., & Yamashita, H. (2003). Muscle type difference in the regulation of UCP3 under cold conditions. *Biochemical and Biophysical Research Communications*, *305*(2), 244–249. https://doi.org/10.1016/s0006-291x(03)00730-7

Wani, A. K., Akhtar, N., Sher, F., Navarrete, A. A., & Américo-Pinheiro, J. H. P. (2022). Microbial adaptation to different environmental conditions: molecular perspective of evolved genetic and cellular systems. *Archives of Microbiology*, *204*(2), 144. https://doi.org/10.1007/s00203-022-02757-5

Whitehead, A., & Crawford, D. L. (2006). Neutral and adaptive variation in gene expression. *Proceedings of the National Academy of Sciences of the United States of America*, *103*(14), 5425–5430. https://doi.org/10.1073/pnas.0507648103

Williams, C. L., Hagelin, J. C., & Kooyman, G. L. (2015). Hidden keys to survival: the type, density, pattern and functional role of emperor penguin body feathers. *Proceedings of the Royal Society B: Biological Sciences*, *282*(1817), 20152033. https://doi.org/10.1098/rspb.2015.2033

Wingfield, J. C., Kelley, J. P., & Angelier, F. (2011). What are extreme environmental conditions and how do organisms cope with them? *Current Zoology*, *57*(3), 363–374. https://doi.org/10.1093/czoolo/57.3.363

Wittkopp, P. J. (2007). Variable gene expression in eukaryotes: a network perspective. *The Journal of Experimental Biology*, *210*(Pt 9), 1567–1575. https://doi.org/10.1242/jeb.002592

Wu, B., Zhang, L., Zhu, Y.-H., Zhang, Y.-E., Zheng, F., Yang, J.-Y., Guo, L.-Y., Li, X.-Y., Wang, L., Tang, J.-M., Chen, S.-Y., & Wang, J.-N. (2018). Mesoderm/mesenchyme homeobox gene l

promotes vascular smooth muscle cell phenotypic modulation and vascular remodeling. *International Journal of Cardiology*, *251*, 82–89. https://doi.org/10.1016/j.ijcard.2017.10.098

Wu, C.-W., & Storey, K. B. (2021). mTOR Signaling in Metabolic Stress Adaptation. *Biomolecules*, *11*(5). https://doi.org/10.3390/biom11050681

Wullschleger, S., Loewith, R., & Hall, M. N. (2006). TOR signaling in growth and metabolism. *Cell*, *124*(3), 471–484. https://doi.org/10.1016/j.cell.2006.01.016

Yang, J., Li, W.-R., Lv, F.-H., He, S.-G., Tian, S.-L., Peng, W.-F., Sun, Y.-W., Zhao, Y.-X., Tu, X.-L., Zhang, M., Xie, X.-L., Wang, Y.-T., Li, J.-Q., Liu, Y.-G., Shen, Z.-Q., Wang, F., Liu, G.-J., Lu, H.-F., Kantanen, J., ... Liu, M.-J. (2016). Whole-Genome Sequencing of Native Sheep Provides Insights into Rapid Adaptations to Extreme Environments. *Molecular Biology and Evolution*, *33*(10), 2576–2592. https://doi.org/10.1093/molbev/msw129

Yeaman, S. (2015). Local Adaptation by Alleles of Small Effect. *The American Naturalist*, *186 Suppl 1*, S74–S89. https://doi.org/10.1086/682405

Yu, G., Wang, L.-G., Han, Y., & He, Q.-Y. (2012). clusterProfiler: an R Package for Comparing Biological Themes Among Gene Clusters. *Omics: A Journal of Integrative Biology*, *16*(5), 284–287. https://doi.org/10.1089/omi.2011.0118

Yu, M., Yue, Z., Wu, P., Wu, D.-Y., Mayer, J.-A., Medina, M., Widelitz, R. B., Jiang, T.-X., & Chuong, C.-M. (2004). The biology of feather follicles. *The International Journal of Developmental Biology*, *48*(2-3), 181–191. https://doi.org/10.1387/ijdb.031776my

Zaefarian, F., Abdollahi, M. R., Cowieson, A., & Ravindran, V. (2019). Avian Liver: The Forgotten Organ. *Animals : An Open Access Journal from MDPI*, *9*(2). https://doi.org/10.3390/ani9020063

Zhang, B., & Horvath, S. (2005). A general framework for weighted gene co-expression network analysis. *Statistical Applications in Genetics and Molecular Biology*, *4*, Article17. https://doi.org/10.2202/1544-6115.1128

Zhao, J., Jiao, Y., Song, Y., Liu, J., Li, X., Zhang, H., Yang, J., & Lu, Y. (2018). Stanniocalcin 2 Ameliorates Hepatosteatosis Through Activation of STAT3 Signaling. *Frontiers in Physiology*, *9*, 873. https://doi.org/10.3389/fphys.2018.00873

Zhuo, Z., Lamont, S. J., Lee, W. R., & Abasht, B. (2015). RNA-Seq Analysis of Abdominal Fat Reveals Differences between Modern Commercial Broiler Chickens with High and Low Feed Efficiencies. *PloS One*, *10*(8), e0135810. https://doi.org/10.1371/journal.pone.0135810

Data Accessibility and Benefit-Sharing

All data pertaining to this study are accessible at the European Nucleotide Archive (ENA) under the study accession PRJEB64484. The Emperor penguin transcriptome can be found under ERS16107788 (HCAY01000001-HCAY01106060). The King penguin transcriptome can be found under the ERS16107787 (HCAX01000001-HCAX01080605). Clean reads from the 3'-QuantSeq mRNA data for each tissue and each species can also be found on the ENA (Study: PRJEB64484) under the sample accessions: ERS16201405 - ERS16201453 (Emperor penguin), and ERS16201454 - ERS16201503 (King penguin). Additional Data including the transcriptome annotations, catalogues of long non-coding RNAs, tissue-enhanced transcripts, and Differentially Expressed Genes (DEGs) per tissue can be found on GitHub at https://github.com/josieparis/EP-KP-transcriptomics, under Zenodo: https://doi.org/10.5281/zenodo.10218729.

Author Contributions

JRP (performed research, analysed data, wrote the paper), FANF (performed research, analysed data, wrote the paper); FP (designed research, performed research, analysed data), SG (performed research, analysed data), MG (performed research, analysed data), AP (performed research), MB (performed research), CC (performed research), LZ (performed research), BH (analysed data), CLB (designed research, performed research, wrote the paper), ET (designed research, performed research, wrote the paper). All authors commented and contributed to the final version of the manuscript.